

Review

Not peer-reviewed version

A Critical Review on Synergistic Integration of Nanomaterials in 3D Printed Concrete: Rheology to Microstructure and Eco-Functionality

[Siva Jamjala](#) , [Manivannan Thulasirangan Lakshmidēvi](#) , [K. S. K. Karthik Reddy](#) , [Bidur Kafle](#) , [Riyadh Al-Ameri](#)

*

Posted Date: 22 September 2025

doi: 10.20944/preprints202509.1821.v1

Keywords: 3D printing concrete (3DPC); nanomaterials (NMs); rheology; microstructural refinement; sustainability



Preprints.org is a free multidisciplinary platform providing preprint service that is dedicated to making early versions of research outputs permanently available and citable. Preprints posted at Preprints.org appear in Web of Science, Crossref, Google Scholar, Scilit, Europe PMC.

Copyright: This open access article is published under a Creative Commons CC BY 4.0 license, which permit the free download, distribution, and reuse, provided that the author and preprint are cited in any reuse.

Disclaimer/Publisher's Note: The statements, opinions, and data contained in all publications are solely those of the individual author(s) and contributor(s) and not of MDPI and/or the editor(s). MDPI and/or the editor(s) disclaim responsibility for any injury to people or property resulting from any ideas, methods, instructions, or products referred to in the content.

Review

A Critical Review on Synergistic Integration of Nanomaterials in 3D Printed Concrete: Rheology to Microstructure and Eco-Functionality

Siva Jamjala ¹, Manivannan Thulasirangan Lakshmidēvi ^{1,2}, K. S. K. Karthik Reddy ¹, Bidur Kafle ² and Riyadh Al-Ameri ^{2,*}

¹ School of Civil Engineering, Vellore Institute of Technology (VIT), Vellore Campus, Vellore 632014, Tamil Nadu, India

² School of Engineering, Deakin University, Geelong, VIC 3216, Australia

* Correspondence: r.alameri@deakin.edu.au

Abstract

The use of nanomaterials (NMs) in 3D printing concrete (3DPC) has shown significant advancements in enhancing both fresh and hardened properties. This review finds that their inclusion in printable concrete has altered the rheological properties of the mix by promoting thixotropy, extrudability, and buildability while simultaneously refining the microstructure to enhance mechanical strength. Additionally, the photocatalytic properties of nano-TiO₂ enable self-cleaning ability and assist pollutant degradation, whereas carbon-based materials improve electrical conductivity, thereby facilitating the development of innovative and multifunctional structures. NMs mitigate anisotropy by filling voids, creating crack-bridging networks, and reducing pore interconnectivity, thereby improving load distribution and structural cohesion in printed structures. Integrating topology optimisation with 3DPC has the potential to enable efficient material usage. Thus, it enhances both sustainability and cost-effectiveness. However, challenges such as efficient dispersion, agglomeration, energy-intensive production processes, high costs, and ensuring environmental compatibility continue to hinder their widespread adoption in concrete printing. This paper emphasises the need for optimised NM dosages, effective dispersion techniques, and standardised testing methods, as well as sustainability considerations, for adapting NMs in concrete printing.

Keywords: 3D printing concrete (3DPC); nanomaterials (NMs); rheology; microstructural refinement; sustainability

1. Introduction

Additive manufacturing in construction, commonly referred to as 3D printing concrete (3DPC), has rapidly evolved from a niche research topic into one of the most disruptive innovations in civil engineering. Its promise of design freedom, material efficiency, reduced labor demands, and enhanced sustainability clearly distinguishes it from conventional concrete construction. Although industries such as pharmaceuticals, medicine, automotive, and aeronautics have already embraced additive manufacturing at scale [1–4], the construction sector is only beginning to unlock its full potential. Over the past decade, global research activity on 3DPC has increased dramatically, with publications expanding more than 72-fold between 2015 and 2024. As illustrated in Figure 1, this steep and continuous rise underscores the accelerating worldwide interest in 3DPC, in line with the scientometric trends reported by Wang et al. [5].

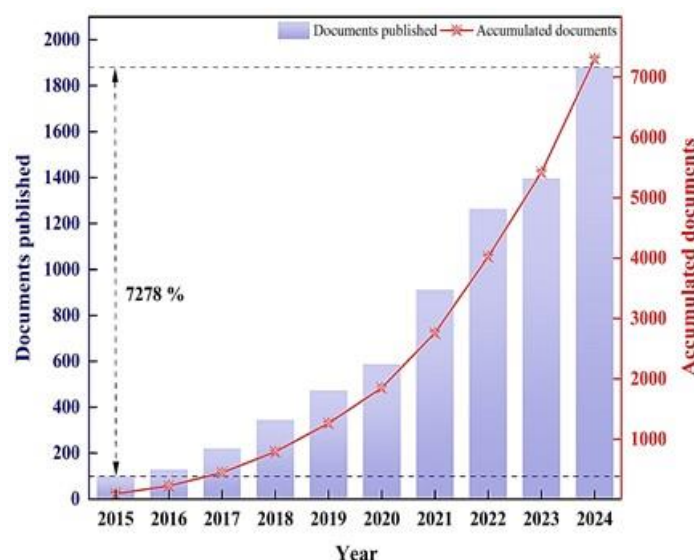


Figure 1. Growth of publications on 3DPC in the Scopus database over the last decade.

3D printing is an automated additive manufacturing technique that fabricates three-dimensional objects from computer-aided design models. In this process, the 3D models are segmented into different two-dimensional layers and then laid down using printers to construct the intended model [6]. Extrusion-based layering (selective material deposition by extrusion) and powder-bed layering (selective binding) are the two main additive manufacturing techniques in the construction sector [7–10].

In the extrusion-based layering process, selected materials are deposited layer by layer using an extrusion print head, guided through computer-aided design tools, which direct the crane, robot, or gantry of a 3D printer equipped with six- or four-axis arms [8,9,11,12]. Examples of extrusion-based printing are contour crafting [13] and concrete printing [1]. The powder-based 3DPC is an additive manufacturing process that creates precise structures by depositing binder liquid into a powder bed and generates detailed geometries through selective deposition, consolidating the powder upon contact with the bed. It is ideal for small-scale building elements, such as panels, formworks, and interior structures, which can be assembled on-site [14].

3D printing technology is being recognised as a pivotal component of the Fourth Industrial Revolution [15]. According to IndustryARC, the global 3D Printing in Construction market is projected to reach approximately USD 205.6 billion by 2030, growing at an unprecedented compound annual growth rate (CAGR) of 113.7% during the forecast period 2024–2030 [16]. The demonstration by NASA of utilising 3D printing for building construction systems on the Moon and Mars highlights the capabilities of 3DPC [17], indicating that the world is ready to transition from conventional concreting to this emerging technology. Its adaptability is further demonstrated through architectural innovation, as shown in Figure 2, where the structural-aesthetic concept of the Bloom installation exemplifies the ability of 3DPC to produce complex, curved, and perforated geometries that merge structural efficiency with aesthetic expression. Collectively, such demonstrations highlight the advantages of 3DPC, such as eliminating formwork that typically contributes 35–60% of concrete cost [18], reduction of 30–60% in construction waste, reduction in labour cost by 50–80%, and cutting down the production time ranging from 50–70% [19]. Additionally, printable concrete adheres to stringent structural imperatives, generates minimal waste, and achieves economic efficiency, positioning it as a forward-looking and responsible alternative to traditional concrete [3,4].



Figure 2. The Bloom structural form, exterior and interior faces [20].

Despite several advantages, 3DPC has a few limitations. Introduction of coarse aggregate, resulting in multifaceted challenges [21], nozzle blockages, emergence of pores [22], impact of printing parameters on mechanical strength of printed specimen [23], lack of reinforcing methods [24], anisotropy [25] and more challenges like cold joints and interlayer bonding are major concerning factors in dragging additively manufactured concrete to establish it as a robust and reliable technique. For instance, Rahul et al. [26], and Chen et al. [27], utilized coarse aggregate in 3DPC and reported an aberration from desired rheological and mechanical properties. For these reasons, numerous researchers exclude the coarse aggregate and employ portland cement along with fine aggregate shown in Figure 3, to achieve the optimal rheological and mechanical properties.

Limited literature [28–32] suggests that other hurdles, such as nozzle blockages and weak inter-transitional zones, can be addressed by developing suitable mix designs that consider factors like the appropriate water-to-cement ratio and aggregate-to-binder ratio. To assist the volume requirement criteria, the production of 3DPC involved the utilisation of a higher dosage of cement and fine aggregate compared to conventional and self-compacting concrete. Consequently, 3DPC exhibits more air voids, primarily due to the absence of compaction during the layer-by-layer deposition process. Although the mix possesses inherent flowability to ensure extrusion and buildability, inadequate control of this property, combined with the lack of compaction, can lead to pore interconnectivity and weak interlayer bonding, ultimately reducing the mechanical performance of printed concrete [33].

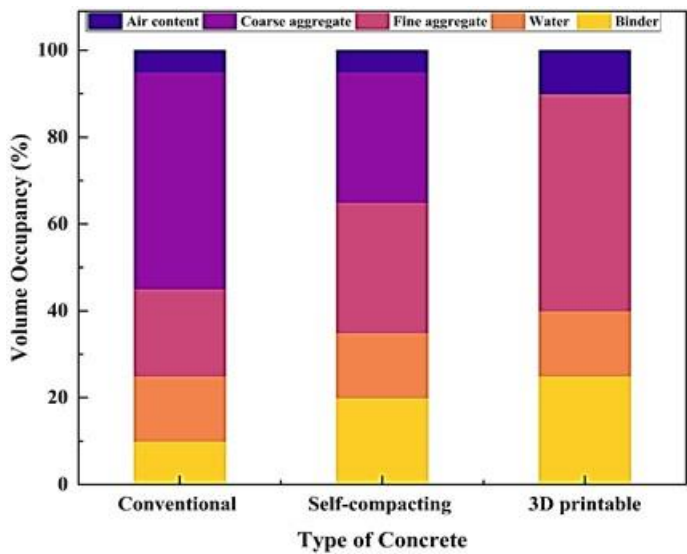


Figure 3. A demonstrative comparison of the proportion of materials by volume consumed in traditional concrete, self-compacting concrete, and 3DPC. Modified from [22].

Along with this, on the other side, there is a parallel pace in enhancing the rheological and mechanical properties of 3DPC by partially replacing cement with micro-sized materials such as silica fume [34,35], rice husk ash [36,37], fly ash [38,39], limestone calcined clay [40–42], GGBS [43] and nano-sized particles like nano clay (NC) [44], nano-silica (NS) [45], nano titanium dioxide (NT) [46], and graphene oxide (GO) sheets [47]. Furthermore, in the investigation of the utilization of nano and micro-sized particle materials in 3DPC [48], nanoparticles exhibited superior performance over microparticles demonstrating enhanced rheological, mechanical, and microstructural properties. This superiority is attributed due to the distinctive reactivity, small size, and expansive surface area of nanoparticles [49]. NMs fill the pores in 3DPC and intensify the microstructural density [50]. Recent investigation by Li et al. [51] highlighted the significance of hydration kinetics and early-age microstructural development in determining the interfacial performance of 3D printed cementitious materials, especially under varying ambient conditions and printing parameters. Following this, a study by Jinwhy et al. [52] demonstrated that the incorporation of hybrid nanomaterials, such as GO and NS, synergistically improved both toughness and crack resistance in 3DPC, owing to their combined effects of hydration nucleation and microcrack bridging. However, careful handling, precise dispersion, and optimal dosage of NMs are essential, as improper use can negatively impact the fresh and hardened properties of concrete. Additionally, a primary challenge associated with NMs lies in the higher production cost [53]. Nevertheless, prevailing research studies indicate that the combination of NMs and micro-sized materials in 3DPC can produce a synergistic effect, resulting in a composition that offers improved performance compared to using each material individually [54–57].

Currently, the demand for a material's viability extends beyond its fundamental sustainability, necessitating a multifaceted approach that aligns with the United Nations' Sustainable Development Goals (SDGs), given the increased environmental impacts, such as global warming and climate change. The construction sector contributes approximately 38% of greenhouse gas emissions, 40% of solid waste production, and 12% of potable water usage and is poised to tackle mounting environmental and socio-economic challenges. Due to the anticipated rise in urban populations, which is expected to represent 68% of the global population by 2050, it is imperative to enhance and adopt innovative, pioneering, and sustainable approaches to cater to the escalating needs for housing, transportation, and essential infrastructure [3]. In this context, there is an urgent need to develop a technology that, unlike traditional construction methods, can improve sustainability. Digital fabrication techniques appear to be a promising candidate, contributing significantly by satisfying 11 out of the 17 SDGs and aligning with broader global objectives for social and economic development. It suggests that 3DPC possesses a diverse range of qualities that make it environmentally sustainable [58]. Currently, the majority of the researchers are developing printable blends only with cement, fine aggregates, mineral and chemical admixtures. Therefore, a higher cement dosage of is essential compared to conventional concrete, acknowledging the elevated carbon dioxide emissions associated with cement production [59] which thereby intensify carbon footprints in the environment through 3DPC [60]. Incorporating a blend of supplementary materials in conjunction with cement presents a promising approach to achieving sustainable development in construction [61]. Sustainable alternatives like recycled powders and reactive fillers have demonstrated potential in reducing the carbon footprint of 3D printed construction, while maintaining comparable mechanical properties [62]. Furthermore, alternative printable mixes developed by geopolymer as a binder [63], alkali-activated material [64] also provide a viable solution for sustainable construction. Nonetheless, the current study focuses on an in-depth exploration of performance of NMs used in 3DPC, where cement is used as a binder system.

Recent reviews [52,65,66] have significantly contributed to the understanding of NMs in 3DPC, particularly about rheological behaviour, early-age hydration kinetics, and the evolution of interfacial zones that govern printability and mechanical fidelity. These efforts have provided foundational insights into the influence of nanoscale additives on flow characteristics, build stability, and mechanical strength, highlighting the importance of material–process interactions. As 3D printing

transitions from formulation development to structural-scale implementation, however, a broader and more integrated perspective is required—one that aligns nanoscale functionalities with macrostructural performance targets, long-term durability, and sustainability objectives.

The present paper provides a comprehensive review of the effect on the rheological, mechanical, and microstructural performance of 3DPC modified with NMs. In the first segment, the role of NMs in enhancing the properties of concrete through various mechanisms, including the filler effect, alterations in hydration kinetics, and microstructural densification, is discussed. It is followed by offering a detailed understanding of fresh and hardened parameters of 3DPC, providing an overview of the material’s behavioural dynamics. In the subsequent sections, an in-depth analysis is presented on the impact of NMs on the overall properties of 3DPC, with an emphasis on the synergistic effects when combined with other SCMs and fibres. Furthermore, the study examines the potential of NMs in promoting sustainable construction practices, with a focus on their adaptability within the emerging field of 3DPC. The studies conclude by examining the role of topological optimisation in enhancing sustainability, emphasising its potential to reduce material usage.

2. Nanotechnology in Cementitious Composites: Influence on Hydration Kinetics, Mechanical Strength and Microstructure

The concept of nanotechnology was first introduced by the renowned physicist Richard Feynman in 1959 through his talk “There’s Plenty of Room at the Bottom” at the American Physical Society meeting at the California Institute of Technology. In his presentation, he emphasised the capabilities of manipulating and governing matter on a microscopic scale, exploring the ramifications and opportunities presented by miniaturisation and nanoscience [67]. After fifteen years, in 1974, another physicist, Taniguchi, coined the term “nanotechnology” [68]. Sobolev et al. [69], disclosed that all materials can be converted to nanoparticles. The effectiveness of nanoparticle formation lies in its ability to impact the purity or fundamental chemical composition of the parent materials. Top-down and bottom-up are the two primary approaches generally used for the synthesis of NMs. In the top-down approach, the bulk material is sliced to create nano-sized particles, whereas in the bottom-up approach, molecules are combined to form larger structures, such as atoms [70,71]. In concrete applications, NMs synthesised through a bottom-up approach are preferred, as they offer precise control over particle size, morphology and specific properties [72]. Figure 4 further classifies the NMs used in concrete based on their composition and dimensional structure, providing a detailed overview of these materials. Figure 5 illustrates their morphology and surface characteristics.

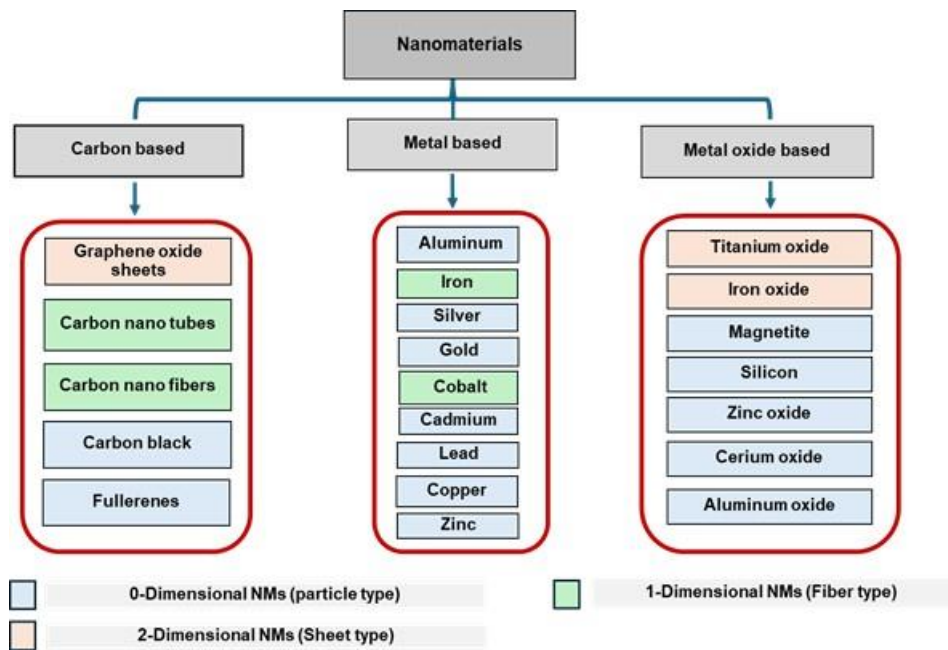


Figure 4. Classification of NMs that are used as a common additive in the conventional and 3DPC according to material composition and by their dimensionality criterion.

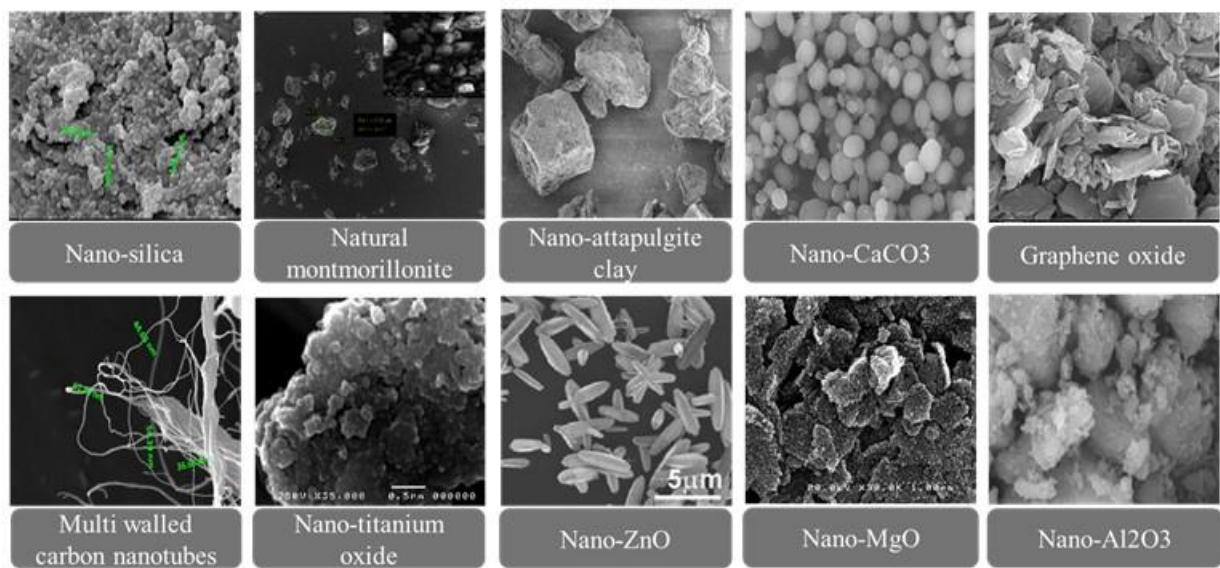


Figure 5. Scanning electron micrographs of various NMs illustrating their morphology and surface texture for use in concrete applications [73–76].

Nanomaterials (NMs), when incorporated into concrete, modify its fresh and hardened behaviour by influencing workability, strength development, durability, and high-temperature resistance, as schematically represented in Figure 6. Active NMs, such as NS, NC, nano-metakaolin, and nano-Al₂O₃, play a pivotal role in influencing the cement hydration reaction. Remaining inert nanoparticles, such as Graphene nanoparticles (GNPs), Carbon nanofibres (CNFs), Carbon nanotubes (CNTs), GO, NT, nano-Fe₂O₃, and nano-ZrO₂, serve as nucleation sites for the precipitation of C-S-H, thereby filling the pores and impeding the formation of microcracks within the concrete matrix [75]. Land and Stephan’s [77] experimentation results also showed that it is possible to accelerate or control the kinetics of cement hydration in multiple ways with the addition of NMs.

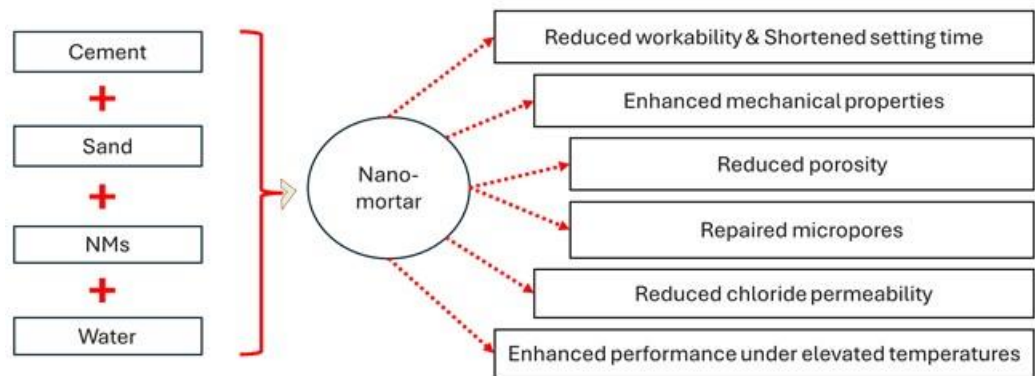


Figure 6. Commonly employed materials in the production of nano-mortar and the enhanced characteristics of mortar by adding NMs. Modified from [78].

Typically, C-S-H gel mainly forms around clinker particles, filling the gaps between them. However, the introduction of C-S-H seeds into the mixture encourages the further growth of C-S-H across the cement matrix, not just surrounding the clinker particles. This seeding procedure yields a

more uniform and compact distribution of C-S-H, thereby reducing porosity and densifying the concrete's microstructure [79].

The evolution of microstructure with hydration time in the plain and NMs-integrated concrete matrix is depicted in Figure 7. Additionally, some NMs, such as NS, nano metakaolin, and nano fly ash, will also form more C-S-H through active pozzolanic reactions and contribute to the improvement of overall mechanical strength. To improve the rheological, mechanical, and microstructural performance of concrete through the addition of NMs to the concrete blend, researchers have begun utilising NMs in printable concrete to enhance the properties and performance of the printed structures.

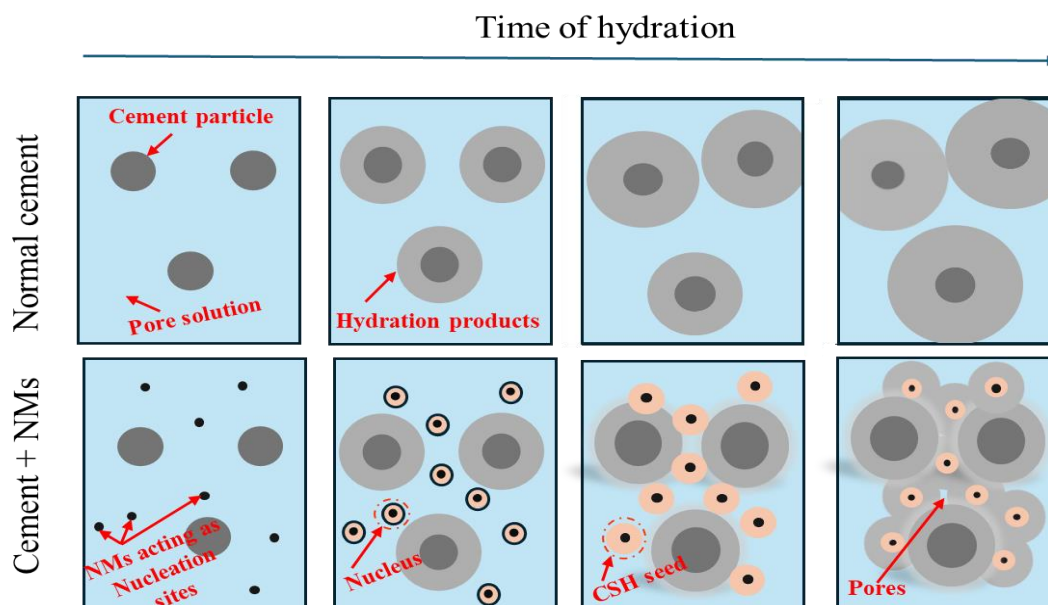


Figure 7. Schematic illustration comparing the evolution of microstructure with respect to time of hydration in a concrete matrix with and without NMs. Modified from [80].

According to Deyu et al. [81], the nucleation effect occurs when a critical ion concentration is reached before the formation of a crystal nucleus and crystal growth in a saturated solution, as described in the classical theory of crystallisation. It represents the stage known as nucleation control in the homogeneous nucleation process of numerous chemical reactions. The utilisation of NMs introduces heterogeneous nucleation, which effectively reduces the critical ion concentration required for nucleation to occur, thereby facilitating rapid crystal growth on the NM surface. For developing ideal cementitious composites modified with NMs, efficient dispersion is necessary due to their small size and high specific surface area, which makes them easily susceptible to agglomerating as clusters in the blend. Therefore, meticulous attention to dispersion methods, such as physical, chemical and physical-chemical, is required [65]. The zeta potential has a significant influence on the electrostatic stability of the colloidal system and governs the dispersion's resistance to agglomeration. Dispersions exhibiting zeta potential values under ± 30 mV are susceptible to quick coagulation and agglomeration due to inadequate electrostatic repulsion. Ultrasonication, a method that utilises cavitation microbubbles to disintegrate agglomerates, is a practical approach to enhance dispersion. Furthermore, adjusting the suspension's pH and applying dispersion strategies, such as the use of surfactants and superplasticisers, can significantly improve stability [82].

Beyond their role in modifying hydration kinetics and microstructure, NMs also provide multifunctional enhancements that directly address the limitations of traditional SCMs, particularly in 3DPC. These materials have emerged as critical modifiers in 3DPC, addressing durability deficiencies stemming from directional porosity and weak interfacial zones formed during layer-by-layer deposition. Compared to traditional SCMs such as fly ash and silica fume, which are typically

added at high dosages (15–30%) and often increase long-term porosity by ~12% while delaying hydration onset, NMs operate more efficiently at significantly lower dosages (0.5–3%) by directly engaging with microstructural degradation mechanisms at the nanoscale through their nucleation potential, filler effects, and chemical reactivity, NMs promote dense hydration products, reduce ion permeability, and fortify weak zones in the matrix and at interlayer interfaces. NS, incorporated at just 1–3% by binder weight, accelerates secondary C-S-H gel formation, thereby reducing chloride diffusion coefficients by 50.8–54.4% and mitigating sulphate-induced mass loss by 16–20% through pore refinement and ion transport resistance [83]. In contrast, silica fume, although reactive, increases paste viscosity and requires up to 20% more super-plasticiser to maintain printability, often complicating rheology in extrusion-based systems [52].

In addition to NS, NT offers multifunctional durability enhancements. At 1–1.5% by cement weight, it reduces average pore diameters from ~100 nm to <50 nm, lowering total porosity by 20–35% and improving chloride resistance by ~30% in ultra-high-performance concrete under flexural stress [84]. Moreover, its photocatalytic activity enables 65–80% NO_x degradation under UV exposure, providing self-cleaning and surface protection in polluted environments [85]. These functionalities are not available in conventional SCMs. GO, even at ultralow dosages (0.06%), forms a hydrophobic, crack-bridging nanonetwork that reduces water absorption by a factor of four and enhances freeze-thaw durability by 68.75%, cutting mass loss from 0.8% to 0.25% across 540 cycles [86]. GO's intrinsic electrical conductivity also supports real-time structural health monitoring, positioning it as a multifunctional additive that far exceeds the capabilities of traditional pozzolans.

The integration of NMs into cementitious composites has revolutionised the design and performance of both conventional and 3DPC. NMs, even at ultra-low dosages, fundamentally enhance hydration kinetics, densify the microstructure, and improve durability by acting as nucleation sites, promoting pozzolanic reactions, and refining pore structure. These additives accelerate C-S-H gel formation, reduce permeability, and impart advanced functionalities, such as self-cleaning and real-time structural monitoring, which are not achievable with traditional supplementary cementitious materials. However, the exceptional reactivity and high specific surface area of NMs demand meticulous dispersion strategies (e.g., ultrasonication, surfactants) to prevent agglomeration and ensure uniform performance gains. Thus, nanotechnology offers a transformative pathway for next-generation concrete, contingent upon precise control of NM dispersion and integration within the cement matrix.

From the above studies, it is clear that the addition of NMs to concrete may enhance its performance by modifying hydration kinetics, microstructural development, and durability. They can act as pozzolanic agents and form additional C-S-H; they can also serve as nucleation sites, promoting heterogeneous crystallisation and densification of the cement matrix. However, dispersion stability, influenced by zeta potential and methods such as ultrasonication, ensures a homogeneous distribution and prevents agglomeration that could undermine the nanoscale mechanisms.

3. Fresh and Hardened Properties of 3DPC and the Role of NMs

3.1. Fresh Properties

Concrete designed for 3D printing requires a delicate balance between high consistency and pumpability. In contrast, the slump test, widely used to assess the workability of traditional concrete, often falls short in detecting subtle variations critical to the performance of printable concrete [87]. Rheological properties in printable concrete offer a more detailed and sensitive characterisation of material behaviour compared to slump tests. However, their assessment typically involves specialised and costly equipment. Although fresh concrete can be readily extruded, its workability or open time for printing is often limited compared to conventional applications [32,88,89]. As viscosity increases over time, workability decreases until the material becomes more rigid, making it suitable for extrusion. Despite the challenges posed by this stiffening, it can enhance the mechanical

strength of the initial layers, thereby supporting the ones that follow. Therefore, rheological measurements are vital for assessing the casting properties of fresh concrete, including workability, flowability, and printability [87].

Furthermore, Prolonged pauses during printing may result in cold joints with weaker bonds between layers. Nevertheless, a structured approach [90] was developed to evaluate pumpability and buildability using slump and slump-flow tests, helping to identify mixtures suitable for 3D printing. Mixes with slump values of 4–8 mm and a slump flow of 150–190 mm were found to provide sufficient buildability and a smooth surface. To illustrate these parameters within the broader context of material behaviour, the classification of fresh properties relevant to 3DPC is presented in Figure 8.

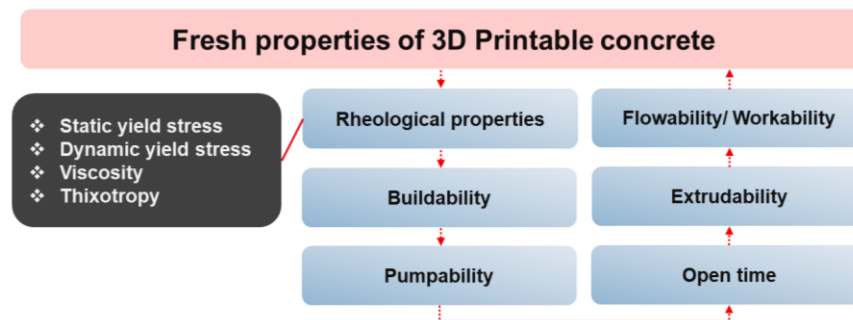


Figure 8. Key fresh properties of 3DPC based on material characteristics.

3.1.1. Flowability

The concept of flowability in 3DPC refers to the ability of the material to deform and be conveyed through the system under pressure while retaining key rheological properties such as yield stress, plastic viscosity, thixotropic recovery, cohesion, and early-age (green) strength during the open time window [11]. If the printable mix possesses high flowability, it is more likely to act as a fluid and adversely affect buildability. Conversely, if the mix is too stiff (i.e., low flowability), it isn't easy to print. Although there is no standard code for the flowability range, a previous study [91], suggested that the mix with a flowability range of 160-200 mm is optimal for printing.

3.1.2. Buildability

Buildability refers to the capability of an extruded material to uphold its form and size even when subjected to continuous and escalating loads caused by the deposition of subsequent layers [92]. It relies on the yield stress of the material, the structural build-up, and the stability of the shape. The initial rigidity is guaranteed by the static yield stress, which ensures that the shape is retained after extrusion before the structural build-up process commences [32,93]. The structural build-up is affected by factors such as flocculation and binder hydration rates [94]. If the material is deposited faster than it builds up, the structure will fail [32]. Buildability failure in 3DPC can occur either through plastic collapse, where stresses exceed the evolving yield strength of fresh concrete, or through elastic buckling, which is governed by material stiffness and elastic modulus in the fresh state [95]. These two primary failure modes are illustrated in Figure 9. There is no standardised test for buildability. However, researchers evaluated buildability by counting the number of printed layers [96], performing a layer deformation test [28], and a cylinder stability test, among others. Perrot et al. [32] analysed the relationship between buildability and static yield stress in layer-by-layer concrete printing using the rheological modelling equation (1) to determine the optimal balance for structural stability and predict failure.

$$H = \frac{\alpha}{\rho g} \tau_s \quad (1)$$

where H (m) is the buildability, α is the geometric factor of the printed structure, ρ is the density of materials (g/cm^3), and g (m/s^2) is the acceleration due to gravity. τ_s (Pa) is the static yield stress.

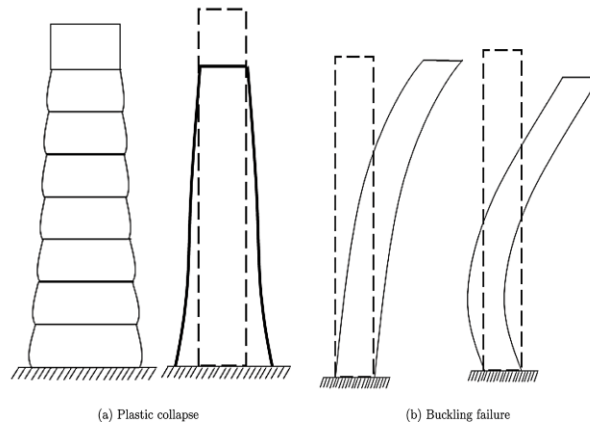


Figure 9. Buildability failure criterion [95].

3.1.3. Extrudability

Extrudability is attributed to how well a printable mix can maintain its dimensional accuracy and layer quality while being continuously extruded through the nozzle [97,98]. Accurate structures are dependent on proper extrusion. To measure this, one can print with fresh material and assess the length without any breakage of printed filament or blockage of the nozzle. Longer uninterrupted length is indicative of superior extrudability [95].

3.1.4. Pumpability

Pumpability refers to the ease with which a printable mix is pumped smoothly through a conduit under pressure and reaches the desired printing location while ensuring its functionality and avoiding segregation [99]. Pumpability is typically assessed indirectly by examining rheological properties, which collectively determine the mix's ability to be pumped efficiently. For ideal pumpability, the viscosity needs to be reduced, while the static yield stress should be increased post-extrusion to enhance buildability. Pumpability in printable concrete should be considered in conjunction with its buildability to ensure a smooth flow through the pump and nozzle while maintaining shape and structural integrity after deposition [100]. In addition, Pumpability, extrudability, and buildability are categorised as the fundamental printable performance criteria for printable concrete [101].

3.1.5. Open Time

In 3DPC, open time refers to the period when the material flows smoothly through the nozzle without any blockages or clogging [102]. The printable mixture must have an open time that exceeds the extrusion time to ensure optimal printability [22]. The test methods employed to assess flowability can also be used to determine the open time of the mixture by examining the flow over time [95]. Furthermore, the cessation of open time is recognised through disruptions in extruded filaments, such as decreased filament width and gaps, which suggest challenges in material extrusion caused by elevated yield stress, leading to blockages in the nozzle [22].

3.1.6. Rheological Properties

The construction material industry introduced rheology to evaluate the initial flow characteristics of materials with composite properties for concrete. Rheology quantitatively analyses and evaluates material characteristics and phenomena, providing a numerical representation of the quality and performance of composite materials in 3D concrete printing [103]. It affects both the fresh

state behaviour and mechanical characteristics of the printed structure; therefore, a thorough comprehension and management of rheological parameters, which include yield stress, plastic viscosity, thixotropy, structuration rate, and flocculation rate, are essential to guarantee the production of high-quality, structurally sound printed concrete elements [22,95].

Yield stress is a fundamental rheological property that determines the material's capacity to maintain its shape after extrusion and impacts the ease of flow during printing. The time-dependent increase in yield stress of fresh concrete is driven by internal structuration and C-S-H formation, which is critical for maintaining the stability and geometrical accuracy of printed structures [101]. Static and dynamic yield stresses are the two types of yield stresses involved in 3DPC. Static yield stress is the minimum stress needed to initiate flow, while dynamic yield stress maintains flow. Higher static yield stress and lower dynamic yield stress are desirable for maintaining buildability and pumpability. Studies [104,105], suggests that an optimal yield stress range of 500 to 2500 Pa is appropriate for 3DPC, with the precise value depending on the specific printing technology and operational conditions. Perrot et al. [32] developed a model (Equation 2) to describe the increase of yield stress over time, considering the structuration rate and time-dependent nature of yield stress, which is not directly a flow model but rather a structuration model. Initially, the strength of concrete increases steadily with age, then shifts to a rapid rise in later stages.

$$\sigma_y(t) = \sigma_{y0} + A_{thix} \cdot t_c \left(e^{\frac{t}{t_c}} - 1 \right) \quad (2)$$

where A_{thix} is the structuration rate, σ_{y0} is the yield stress at $t = 0$, and t_c is the curve-fitting parameter derived from experimental data.

Thixotropy is a reversible rheological behaviour exhibited by printable concrete. When an external shear force is applied, the concrete loses its flocculated structure and starts to flow. Upon the reduction or removal of the shear force, the concrete ceases to flow, and the particles begin to flocculate again due to interparticle interactions. This process restores the static yield stress of the mix. Thixotropy describes the material's ability to transit between a fluid-like state when sheared and a solid-like state when the shear is reduced or removed, ensuring the concrete can be easily shaped during extrusion and regain its strength afterwards [91]. The behaviour of concrete can be assessed through experimental tests, such as hysteresis loops, incremental variations in shear rate or shear stress, dynamic moduli, and start-up or creep tests [19]. Kruger et al. [106] developed a novel analytical model where they presented a bi-linear thixotropy model, incorporating indices such as R_{thix} (Re-flocculation rate) and A_{thix} (Structuration rate/ Structural build-up rate) further reported that R_{thix} in particular is significant because it measures the material's ability to regain its internal structure after shear quickly, ensuring stability and facilitating the addition of new layers, which is essential for maintaining the integrity of the printed structure throughout the building process.

Plastic viscosity (μ_p) is another notable rheological property of printable concrete, referring to the additional shear stress required to increase the flow rate [107]. It is essential for a seamless 3D printing process and for maintaining the structural integrity of the material after it has been extruded. Rotational rheometers are used to measure it, working in conjunction with yield stress to describe the overall rheological behaviour of printable concrete in its fresh state [91].

The rheological behaviour of 3DPC is typically characterised using the Bingham plastic model, as described in Equation 3, which considers concrete as a Viscoplastic material. This model is widely used by many researchers due to its simplicity [108]. However, the Herschel-Bulkley model in Equation 4 and the Power-law model in Equation 5 can also be utilised to determine the yield stress and plastic viscosity of printable concrete. Prem et al. [109] validated the three models mentioned above. They reported that all models adequately predicted the rheological properties of printable mixes with components such as NS, Polyvinyl alcohol fibres, and fly ash. Furthermore, the authors suggested that further studies are needed to identify the most suitable model to reduce extensive experimentation.

$$\tau = \tau_0 + \mu_p \dot{\gamma}, \tau > \tau_0 \quad (3)$$

$$\tau = \tau_0 + K\mu_p \dot{\gamma}^n, \tau > \tau_0 \quad (4)$$

$$\tau = K\dot{\gamma}^n \quad (5)$$

where τ is shear stress, τ_0 is yield stress, μ_p is plastic viscosity, $\dot{\gamma}$ is the shear rate, and n is the flow index.

To maintain structural integrity, the internal structural buildup of the lower layer must be greater than the stress due to the gravitational load or self-weight of the upper layer, which is printed or about to be printed; otherwise, the layers will settle and lead to collapse. Together, these rheological parameters determine the fresh-state performance of 3DPC, linking fundamental material behaviour to practical outcomes such as pumpability, extrudability, buildability, and shape stability. This relationship is conceptually illustrated in Figure 10.

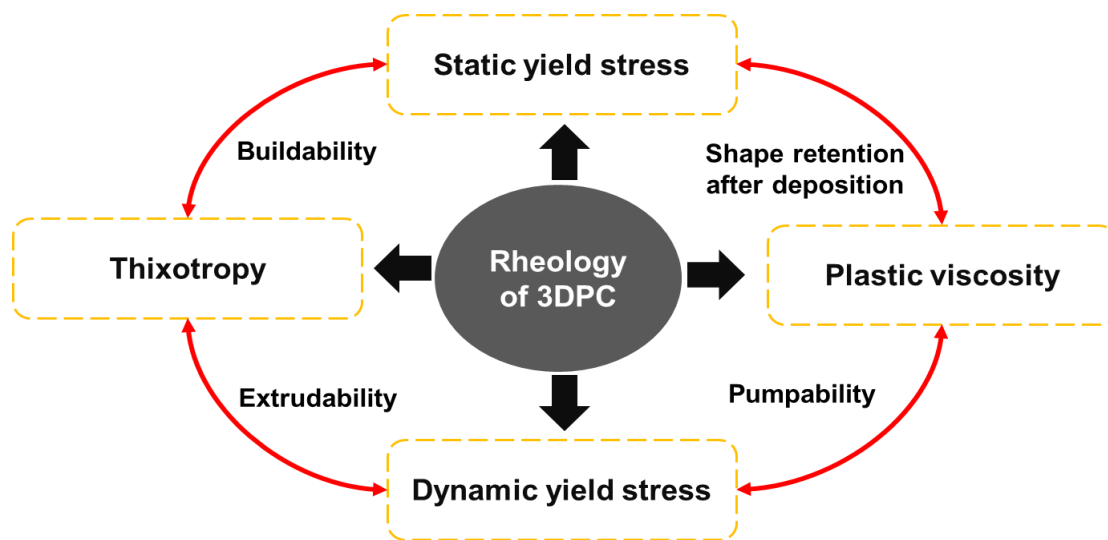


Figure 10. Conceptual framework of fresh performance of 3DPC.

In NM-enhanced 3D printable cementitious systems, hydration begins almost immediately after mixing due to the presence of highly reactive NMs such as NS, NC, and Nano Calcium carbonate (NCa). These additives act as nucleation sites, significantly accelerating the formation of C-S-H and reducing the induction period of cement hydration. This early-age acceleration leads to swift structural build-up and increased matrix cohesion, both of which are critical for maintaining geometric fidelity during the layer-by-layer printing process [46]. These materials also enhance thixotropy by promoting reversible flocculation, allowing the material to flow under shear during extrusion but rapidly regain stiffness after deposition, thus supporting the stability of subsequent layers [52]. Quantitative assessment of these effects involves both conventional tests (e.g., mini-slump, flow table) and advanced rheometric techniques that provide detailed insights into yield stress, plastic viscosity, and thixotropic index. Uniform dispersion, typically achieved using ultrasonication or high-range water reducers, is crucial for maximising nanoparticle effectiveness and preventing agglomeration [50]. Overall, tailoring nanomaterial content and dispersion strategies enables precise control over fresh-state properties, directly translating into improved printability, structural integrity, and process reliability in 3DPC.

3.2. Mechanical Properties

Interlayer bond strength is a distinctive mechanical property of 3DPC, absent in conventional cast concrete, and plays a critical role in ensuring structural integrity. If not adequately managed, weak interlayer bonding can lead to the formation of cold joints. But there are no existing norms for testing this property [95]. Researchers determine interlayer bond strength by applying a tensile load perpendicular to the deposited layer [8], using two loads in opposite directions (longitudinal) on the deposited layers [110] and split tensile test [111]. Few researchers [8,112] have found that interlayer bond strength is closely associated with the printing time gap and the amount of moisture available on the surface. With the increase in the printing gap, the tensile bond strength will decrease.

While these experimental evaluations offer valuable insights, they also highlight the inherently anisotropic nature of 3DPC and underscore the need for predictive modelling frameworks to inform structural design. Recent advances in constitutive modelling have enabled a more precise understanding of the anisotropic mechanical behaviour inherent to 3DPC. The layer-by-layer deposition process produces a laminated, orthotropic microstructure, resulting in direction-dependent stiffness and strength properties. Experimental and modelling studies have confirmed that the print direction significantly influences the load-bearing capacity and failure modes of 3D-printed structures, necessitating specialised constitutive laws to capture this anisotropy [111]. To address this, new orthotropic damage-plasticity models have been developed, extending classical isotropic formulations to account for the nonlinear, irreversible deformations and stiffness degradation observed in 3DPC. For example, Mader et al. [113] introduced a computationally efficient orthotropic damage-plasticity model, validated through finite element simulations and experimental tests with varying print orientations, which accurately replicates the directional dependency of mechanical response. These advanced models are crucial for predicting the structural performance of complex geometries and optimising design parameters in additive manufacturing workflows.

4. Influence of NMs on Fresh and Hardened Properties of 3DPC

4.1. Nano Silica

Numerous studies have investigated the incorporation of silica nanoparticles in conventional and 3DPC, consistently highlighting their ability to enhance both rheological properties and mechanical performance. The superior pozzolanic reactivity of NS enables it to alter the hydration kinetics, offering significant benefits for the long-term performance of cementitious materials. According to Senff et al. [114], the presence of NS accelerates hydration by establishing nucleation sites for the precipitation of C-S-H gel, thereby leading to potential modifications in the static yield stress due to variations in initial hydration reactions and the physical characteristics of the system. Specifically, NS provides a significantly larger surface area for hydration reactions compared to traditional cement particles, thereby enhancing the rate and extent of C-S-H gel formation, which results in a more compact microstructure and a reduction in pores. These findings are supported by Quercia et al. [115], who emphasised that the higher surface area of NS, coupled with its function as a nucleation site, plays a pivotal role in the transformations witnessed within cementitious systems; these modifications affect the hydration kinetics, which in turn influence the static yield stress of fresh concrete.

Qiang et al. [116] investigated the effects of various mineral admixtures, including fly ash, ground slag, silica fume, NCa, attapulgite, and NS, on the rheological properties and structural development in cement pastes. They reported that NS has shown better rheological behaviour, significantly improving C-S-H formation, static yield stress, and overall performance compared to other additives, such as silica fume, fly ash, and ground slag. At optimal dosages (1–2%), NS demonstrated superior mechanical efficiency and hydration kinetics, particularly at lower w/c ratios. Oscar et al. [45] evaluated the influence of NS, micro silica, metakaolin, and nano calcium carbonate in 3D printable cement pastes. In their experimental study, NS outperformed all other materials due

to its enhanced buildability, smooth extrusion and higher thixotropy. Additionally, both NS and NC reduced pore volume by up to 16.2% and increased the hydration product volume fraction by 4.3%. This progressive improvement in buildability with increasing NS content is further illustrated in Figure 11, where the inclusion of NS markedly enhanced layer stability and vertical shape retention. Notably, the mix with 1% NS achieved a 133% increase in the number of printable layers compared to the reference mix without NS, demonstrating significantly higher build heights and improved overall structural integrity as the dosage of NS increased [117].



Figure 11. Buildability of printed elements with increasing NS content. Modified from [117].

Kruger et al. [118] developed a thixotropic model that incorporates re-flocculation and structuration rates to assess the suitability of the material for 3DPC. Rapid re-flocculation is crucial for maintaining the material’s shape immediately after deposition, thereby enhancing its strength after extrusion. The structuration rate quantifies the increase in static yield stress over time, driven by chemical processes such as the formation of ettringite needles. The incorporation of NS enhances re-flocculation, thereby improving buildability without sacrificing structural integrity; however, an excess of NS may negatively impact thixotropic behaviour. The research highlights the importance of optimising the dosages of NS and superplasticisers to expedite the development of static yield stress, ensuring quicker structural stability and facilitating higher printing speeds. A comparative analysis of existing rheological models, including the Bingham, Herschel-Bulkley, and Power-law models, was conducted by Prem et al. [109] to identify the most suitable prediction model. The study investigated the effects of varying dosages of nano-silica, polyvinyl alcohol fibres, and fly ash on the mix’s flow characteristics. All models provided valuable insights into the rheological behaviour of mixes, with the Herschel-Bulkley model offering slightly higher reliability. Nonetheless, the study highlights the need for continued refinement of these models to further enhance their accuracy and relevance for diverse 3D concrete printing applications.

Jacques et al. [119] studied the effects of silica and silicon carbide nanoparticles on high-performance 3D printable concrete. The addition of NS reduced re-flocculation rates by nearly 48% and structuration rates by 33%, while silicon carbide achieved reductions of 42% and 24%, respectively. The highest compressive strength of 80.3 MPa was observed at 1% NS, while 2% yielded the best flexural strength of 9.2 MPa, with higher dosages leading to diminishing returns. Silicon carbide exhibited inconsistent trends in compressive strength, and while NS increased stiffness, silicon carbide caused slight reductions in Young’s modulus. Both nanoparticles enhanced buildability and thixotropy, but silicon nanoparticles showed superior improvements in structural stability during printing. Another study [120] was conducted by adding nano-SiC and reported that the continuous addition of nano-SiC significantly increased both static and dynamic yield stresses, reaching peaks of 6483 Pa and 2803 Pa, respectively, indicating improved initial resistance to deformation. However, the re-flocculation and structuration rates decreased with higher nano-SiC content, dropping to 4.2 Pa/s and 0.61 Pa/s, respectively, indicating a reduced ability of the cement paste to rebuild its internal structure after shearing, which leads to diminished thixotropic behaviour. Mechanical properties, such as compressive and flexural strengths, reached their peak at a 3% nano-

SiC addition. Scanning electron micrograph analysis revealed that nano-SiC effectively reduced microstructural voids and crystal sizes, resulting in a denser microstructure and improved mechanical performance.

Beyond rheology and buildability, NS also plays a role in influencing anisotropy in 3DPC. Qian et al. [121] reported that compressive strength varied between cast specimens and those printed in the X- and Z-directions, confirming the anisotropic nature of 3DPC. They attributed this directional dependence to interlayer bonding and filament alignment, and further showed that even at low dosages (0.5–1%) NS, particularly when combined with polypropylene fibres, significantly reduced the anisotropic coefficient. These findings highlight the dual role of NS in improving material performance while also emphasising the need to optimise mix design and printing strategies to minimise strength variations across different orientations.

4.2. Nano Clay

Nano clays, which are nanoparticles of layered mineral silicates such as montmorillonite, bentonite, and kaolinite, exhibit unique properties including high chemical reactivity, stability, and significant hydration and swelling capacity due to their platelet structure (≈ 1 nm thick, 70–150 nm wide). They form interactions with cement particles to create a dense microstructure [122]. During shear, Van der Waals bonds break but can reform after deposition; this can cause a long structural recovery time; adding NC strengthens particle interactions because of its charged edges and thixotropic behaviour, as shown in Figure 12.

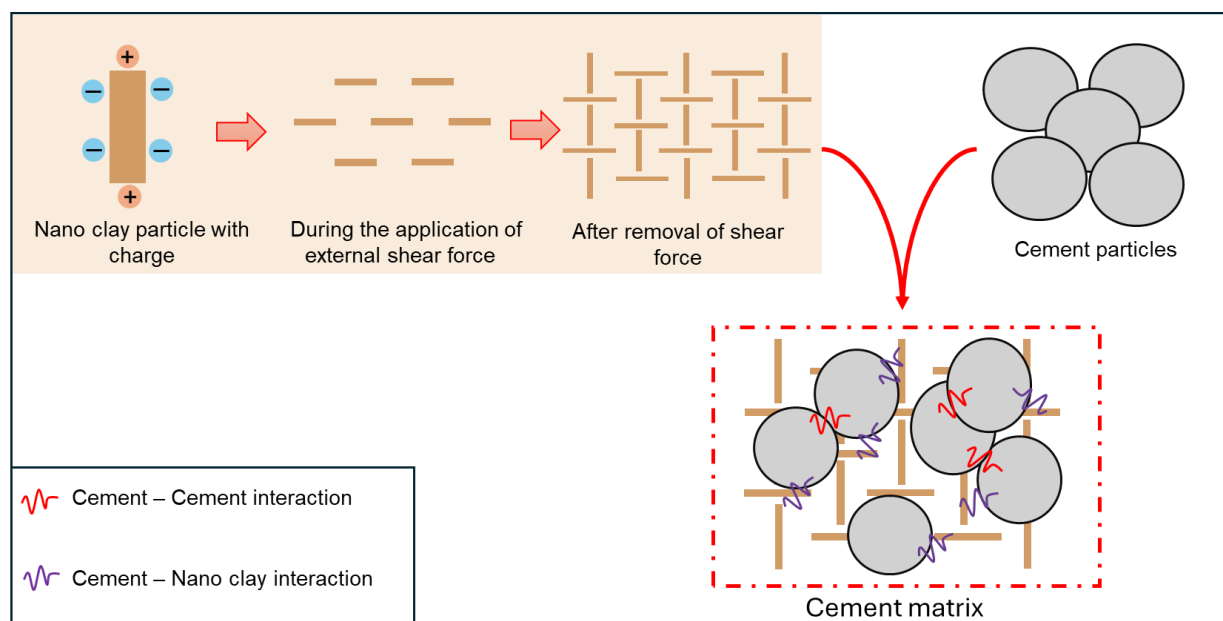


Figure 12. Behaviour of NC particles during and after the removal of external shear force with time. Modified from [123].

The thixotropic effect of NC is further confirmed by Panda et al. [75], who reported that the incorporation of nano attapulgite clay significantly increased yield stress, apparent viscosity, and structural build-up rates, thereby improving printability, as shown in Figure 13. Owing to these rheological improvements, NC is widely employed in extrusion-based 3DPC, where it primarily functions as a viscosity-modifying agent (VMA).

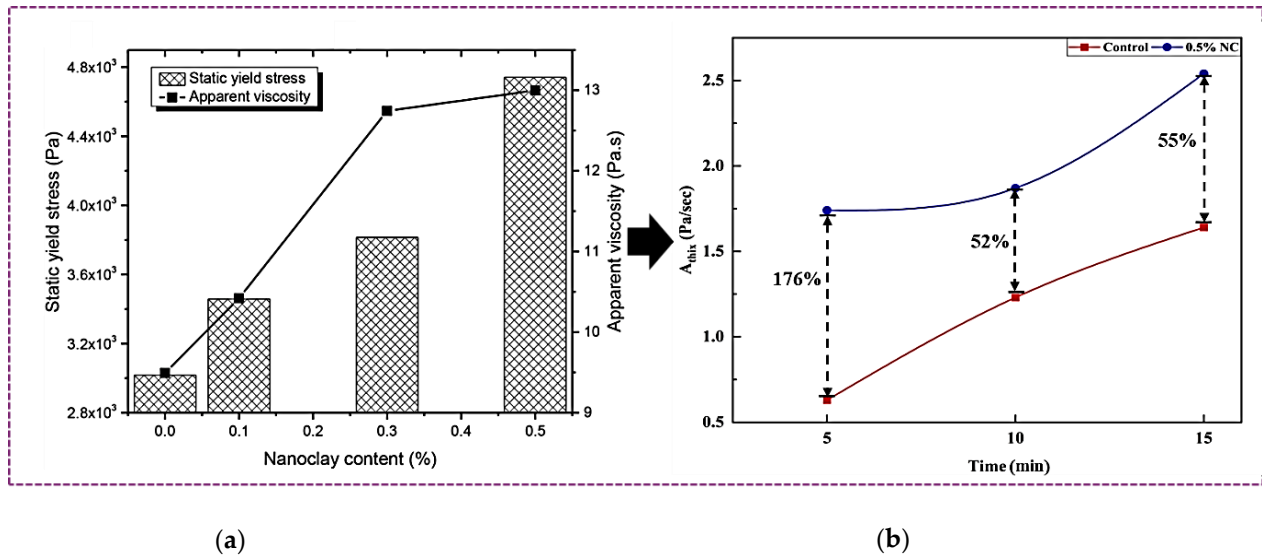


Figure 13. Influence of NC on rheological properties (a) Static Yield Stress (b) Apparent Viscosity [75].

Kaushik et al. [56] investigated the influence of NC on the fresh properties of 3DPC. They found that the addition of NC reduced the slump flow by 20% (Figure 14), while increasing the yield stress by over 60%, indicating enhanced cohesiveness, stability, and printability of the blend. The study highlighted a strong inverse relationship between slump flow and yield stress. Notably, the addition of NC enhanced the elastic modulus at an early stage, improving the green strength of the mortar. This enhancement is attributed to the formation of calcium silicate hydrate, which accelerates the development of early strength. Hugo et al. [124] investigated the effects of three different types of clays—bentonite, sepiolite, and attapulgite—combined with two kinds of VMAs and fly ash on the rheological properties of cement-based systems for 3D printing. The study found that sepiolite, when paired with methylcellulose ether as a VMA, significantly enhanced extrusion characteristics by doubling the initial shear yield stress, achieving values above 2 kPa for defect-free extrusion. While fly ash reduced the paste's thixotropy, sepiolite mitigated this effect and improved the structural build-up rate to 155 Pa/min. Methylcellulose ether-based VMA increased cohesion and extrudability but delayed stiffening, highlighting the importance of balancing initial and compressive yield stresses for optimal buildability. Proper extrusion is associated with a cohesive mixture and low friction. The study also reported that the cone penetration test, though helpful in assessing extrusion and buildability, was observed to overestimate shear yield stress over time due to compression effects during testing. Further studies [125,126] have confirmed the above-reported findings, indicating that the inclusion of NC in the printable mix improves yield stress and thixotropy, leading to better structural rebuilding rates and reduced formwork pressure.

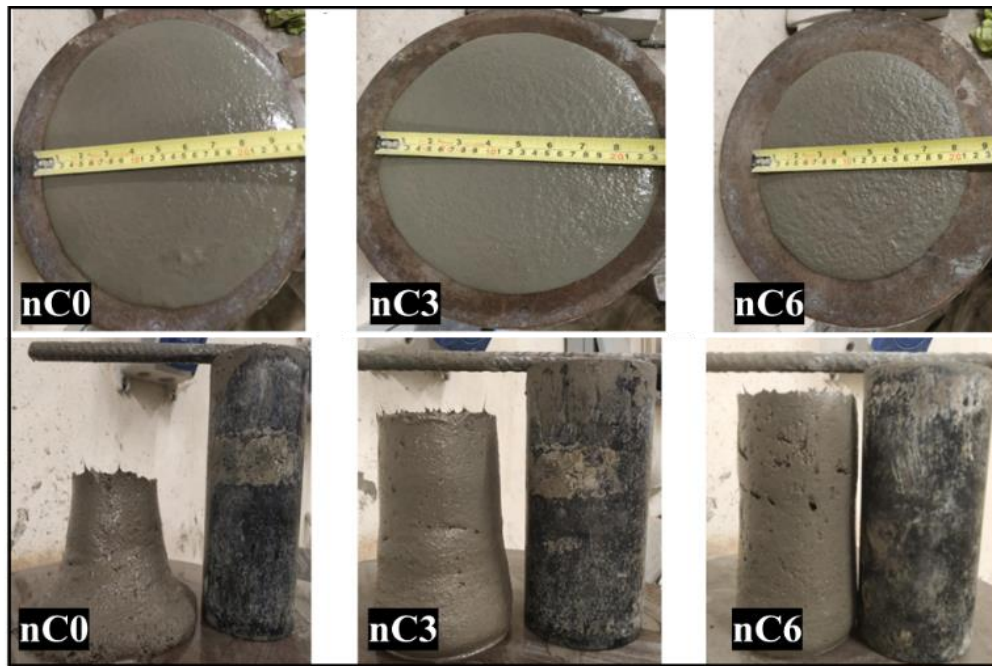


Figure 14. Reduced spread diameter and improved slump stability with increasing NC dosage [56].

Rahul et al [105] reported that incorporating 0.1–0.3% NC enhanced thixotropy and yield stress control, improving buildability. Yu Wang et al. [127] investigated the effects of NC addition at 7–9%, revealing its role as a nano-filler that bridges the gaps between cement particles, thereby forming an interlocking microstructure. Thus, it improved static yield stress by 1.5–2 times while boosting green strength by 20–30%. A synergistic effect with 3% superplasticiser doubled the initial yield stress, achieving optimal extrusion with a fluidity of 170–200 mm and a viscosity that rose from 1.6 to 2.6 Pa·s. Sonebi et al. [54] reported that incorporating NC enhances the cohesiveness and flocculation strength of printable concrete, increasing density and yield stress, though varying proportions may compromise workability and extrusion properties. Kaushik et al. [44] optimised NC incorporation by defining a “printability box” to balance static yield stress and consistency. The 3% NC mix achieved an ideal synergy of workability and structural stability, ensuring cohesive, sharp, and segregation-resistant layers.

Ali et al. [28] and Zhang et al. [55] studied the effects of NC and SF on the workability and printability of printable concrete. Ali et al. found that incorporating 0.3% highly purified attapulgite clay and 10% SF improved compressive strength by 10%, with NC showing the least layer settlement. SF enhanced print quality and shape stability. In contrast, Zhang et al. reported that adding 2% NC and 2% SF significantly improved buildability, with the double-doped blend increasing buildability by four times and green strength by two times compared to the reference mix. Both studies highlighted a linear inverse relationship between green strength and flowability, emphasising the challenge of balancing structural integrity with extrusion ease in 3D printing applications. A study [128] investigated low-carbon 3D printed concrete by incorporating 50% GGBS and highly purified attapulgite nano clay at 0.25% and 0.5% by mass of cement. The results indicated that mixes with only cement demonstrated mechanical properties that were over 50% higher compared to those containing GGBS. However, the addition of NC reduced this decline to less than 10%. Although GGBS provides a sustainable pathway to reducing embodied carbon, its optimal replacement levels require further study to ensure reliable printability.

NC also influences hardened properties by accelerating strength gain, enhancing elastic modulus, and inducing anisotropic variations in compressive and flexural strength [75,129,130]. In synergy with SCMs, it promotes early strength development and long-term densification. Its effectiveness, however, is dosage-sensitive: moderate levels stabilise the mix and strengthen

interlayer bonding through ettringite networking, whereas excessive amounts sharply increase viscosity and hinder extrusion.

4.3. Nano CaCO₃

Calcium carbonate nanoparticles are one of the most affordable nanoparticles available. It is because of its lower energy-intensity requirements for manufacturing [131]. They are widely used in cement-based materials because of their significant physical and chemical reactivity, as well as their compatibility with various matrices. Additionally, CaCO₃ nanoparticles are non-toxic to both humans and the environment, making them a more sustainable and eco-friendly option [132].

In a study conducted by Yang et al [133], the authors partially replaced limestone powder in printable blends with 1-3% CaCO₃ nanoparticles by mass, highlighting that the incorporation of NCa improved buildability without significantly affecting flowability. The nucleation effect of NCa accelerated hydration, resulting in enhanced green strength and yield stress. Notably, the addition of 3% NCa reduced layer deformation by nearly one-third compared to the 0%, 1%, and 2% blends, indicating improved buildability. While mechanical properties, such as compressive and flexural strength, showed limited improvement, the compressive strength of the 1% NCa mix outperformed that of the other blends. However, the compressive strength remained lower than that of cast specimens due to the presence of elongated voids, which reduced the overall mechanical strength. NCa accelerates cement hydration and enhances the microstructure by increasing density and reducing pore size. In another study [134], the incorporation of calcium carbonate nanoparticles at a 1–4% mass fraction as a partial replacement for fly ash significantly enhances the rheological, mechanical, and microstructural properties of printable concrete. The filler and hydration-accelerating effects of NCa refine the pore structure, increase yield stress and viscosity, and reduce vertical filament displacement, improving stability during printing. At 2%, NCa achieves an optimal balance between rheology and strength. Mechanical properties peak at 4%, with compressive strength doubling from 25 MPa to 50 MPa and flexural strength rising from 8 to 13 MPa. SEM and BSE analyses confirm a denser microstructure, smaller calcium hydroxide crystals, and uniform distribution of hydration products, emphasising NCa's role in refining the microstructure and enhancing performance.

NCa demonstrates significant potential in 3DPC by enhancing properties such as buildability, yield stress, and microstructure through hydration acceleration and pore refinement. However, its influence on mechanical properties, such as compressive strength, is inconsistent and often impacted by printing-induced voids and anisotropy. While its eco-friendliness and cost-efficiency make it an attractive choice, research on its comprehensive performance in both fresh and hardened states remain limited, necessitating further exploration for full-scale applications.

4.4. Carbon Based Nanomaterials

Carbon-based nanomaterials have been extensively investigated as reinforcement fillers in cementitious composites due to their unique properties. A detailed classification of these materials is presented in Figure 4. However, additional types exist beyond those illustrated, highlighting the diversity. These materials provide a bridging effect, resist crack propagation and accelerate hydration reactions. Furthermore, the specific porous and layered structures of these materials function as viscosity-modifying agents capable of altering the rheological behaviour required for 3DPC [52]. A detailed analysis of some of these materials is provided in the subsequent sections.

4.4.1. Carbon Nanotubes and Fibers

Sun et al. [135], added multi-walled carbon nanotubes (MWCNTs) and polyvinyl alcohol fibres at maximum dosages of 0.1% for the former and 1.5% for the latter by mass of binder. The study highlighted that the addition of MWCNTs did not result in any noticeable variation in flowability, setting time, or buildability. In contrast, the addition of fibres drastically reduced flowability by

around 40% and made the mix stiffer to extrude. The compressive strength and flexural strength were not significantly different after 28 days, and no clear trend patterns for strength development were observed. It was concluded that the excessive agglomeration of MWCNTs may be the cause of this phenomenon. Nevertheless, the addition of fibres demonstrated a bridging effect in the specimen.

In contrast, Ali et al. [57], dispersed MWCNTs using sonication and showed that proper dispersion is critical. Their results highlighted that 0.2% CNTs improved buildability by 81% and that a combination of 5% silica fume and 0.1% CNTs increased buildability by 74% compared to the reference. Furthermore, 0.2% CNTs enhanced compressive strength by 72%, Young's modulus by 43%, and nearly doubled flexural strength after 28 days. This improvement was linked to nanoscale crack bridging, where CNTs form fibre-based networks that reduce macrocracks and voids. The scanning electron micrographs in Figure 15 show CNTs bridging within the cement matrix at different dosages, highlighting the importance of effective dispersion versus agglomeration.

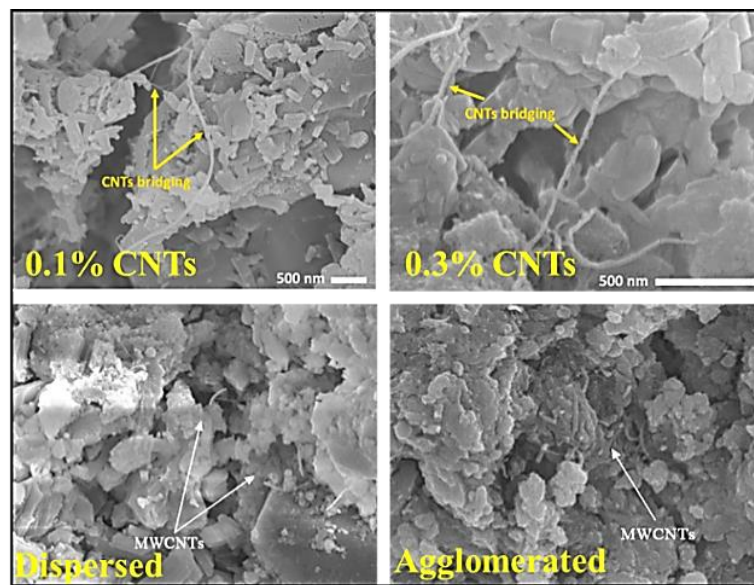


Figure 15. CNT dispersion and bridging in cementitious composites: (top) bridging at 0.1% and 0.3% CNTs, (bottom) comparison of dispersed and agglomerated MWCNTs [57,135].

CNFs have been explored as functional additives to enhance the electrical performance of 3D-printed cementitious composites. Goracci et al. [136] reported that incorporating CNFs increased the electrical conductivity of 3D-printed specimens compared with mould-cast counterparts, with conductivity improving in direct proportion to CNF content. The superior performance of printed concrete was attributed to the extrusion process, which aligns fibres along efficient pathways, while also modifying the pore network to improve the distribution and retention of free water molecules, thereby facilitating ion transport. This alignment also enhanced the longitudinal-to-transverse conductivity ratio, providing directional conductivity that is beneficial for applications such as sensors and conductive composites. Complementing this, Kosson et al. [137] observed that CNF- and CMF-modified mixes suffered from under-extrusion issues and that CNFs reduced compressive strength by 44% compared with controls, underscoring the trade-off between conductivity and mechanical performance. As illustrated in Figure 16, electrical conductivity increases with CNF content up to an optimal dosage, after which agglomeration reduces efficiency, particularly in mold-cast specimens.

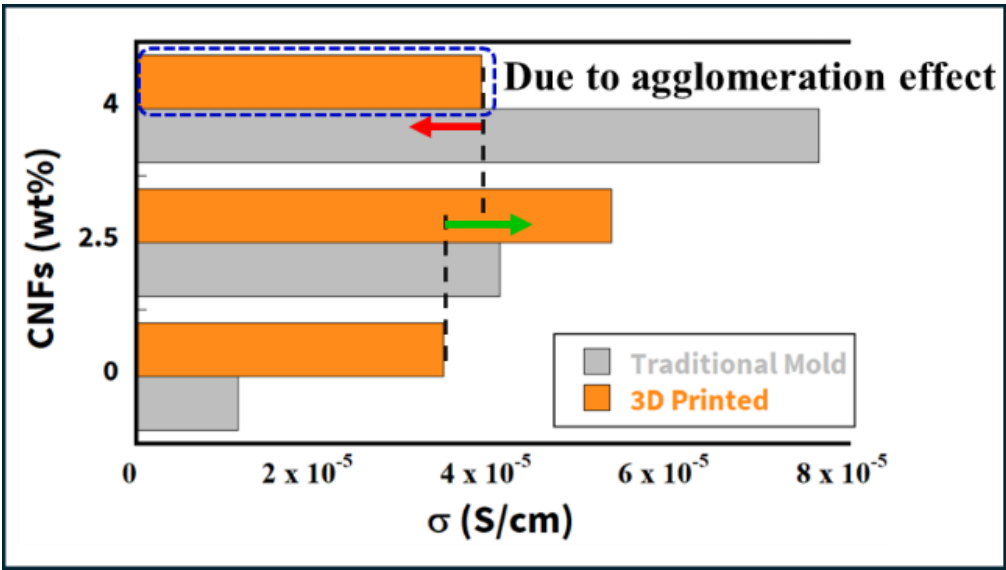


Figure 16. Effect of CNF dosage on electrical conductivity of 3D-printed and mold-cast composites [136].

Collectively, these findings show that while CNTs enhance buildability and mechanical properties through nanoscale crack bridging, CNFs provide directional conductivity and multifunctional potential. However, issues such as agglomeration, nozzle blockage, and inconsistent strength gains highlight the need for precise dispersion methods and dosage optimisation to fully explore their benefits.

4.4.2. Nano Graphene Oxide

Liu et al. [47] investigated the incorporation of graphene oxide (GO) sheets in 3DPC and reported that a 0.015% dosage (by binder mass) increased compressive strength by ~10%, attributed to effective dispersion and matrix filling. In contrast, 0.03% GO reduced flowability, which caused void formation and weakened strength despite microstructural densification at both dosages. Notably, the influence of GO is also direction-dependent: as illustrated in Figure 17, a 0.015% dosage improved compressive strength along all loading directions, whereas 0.03% reduced the gains and amplified anisotropy. This highlights the importance of dosage optimisation to balance workability and mechanical performance.

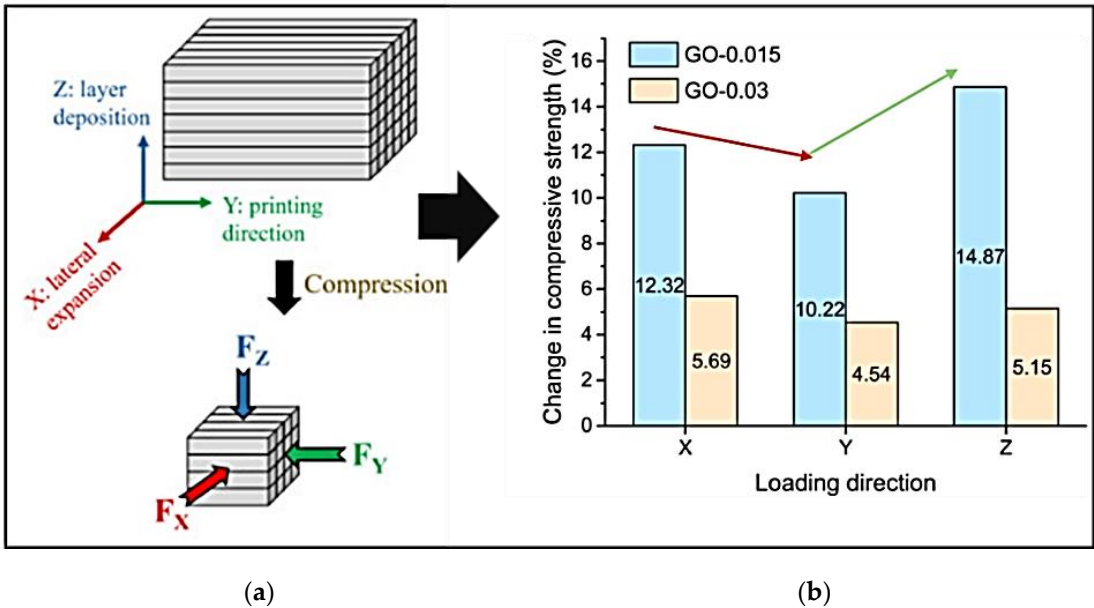


Figure 17. (a) Direction of compression strength testing (b) Effect of GO dosage on compressive strength in different loading directions [47].

Further study by Ahmadi et al. [138] confirmed the mechanical benefits of graphene modifications, where GO-coated steel fibres yielded a 20% gain in compressive strength, doubled tensile strength, and 60% higher flexural strength, alongside narrower cracks under flexural loading. These results reinforce the structural potential of GO when dispersion and fibre integration are well controlled.

Dulaj et al. [139] examined the influence of GNPs on the mechanical and self-sensing performance of 3DPC. While GNPs improved compressive strength and self-sensing ability in cast specimens, their impact on printed ones was strongly affected by anisotropy from layer-by-layer deposition. As shown in Figure 18, printed specimens exhibited direction-dependent resistivity responses: in Direction 1, the addition of 1.2% GNPs increased the resistivity change from 19.3% to 35.5%, whereas in Direction 2, the gain was smaller (22.8% to 25.8%). This highlights that although GNPs can enhance self-sensing ability, their effectiveness in printed elements depends on the printing orientation and interlayer bonding quality.

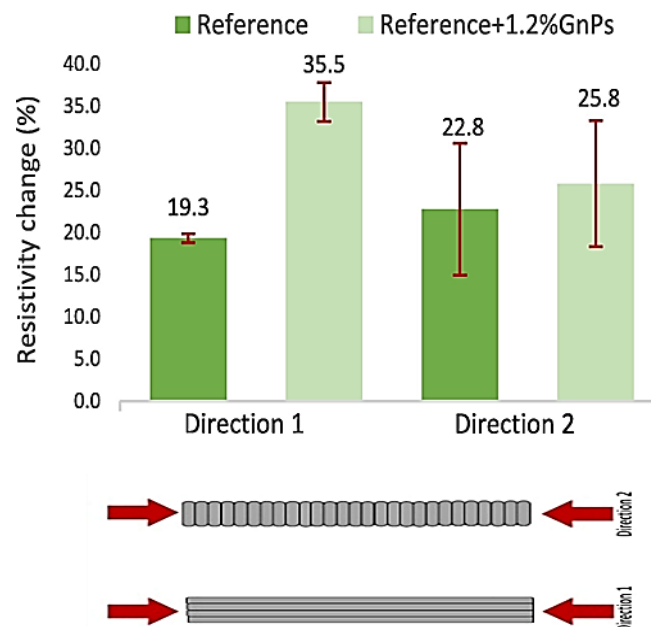


Figure 18. Resistivity change in printed mortar specimens with and without GNPs tested along two printing directions [139].

Taken together, these studies indicate that GO nanoparticles and GNPs have strong potential to enhance the mechanical properties and multifunctionality of cementitious composites. However, their use in 3DPC is limited by challenges such as reduced flowability, agglomeration at higher dosages, and weaker interlayer bonding. Overcoming these barriers requires careful dosage optimisation, improved dispersion methods, and the integration of admixtures to balance mechanical performance with printability and structural integrity.

4.5. Nano TiO_2

Titanium dioxide nanoparticles possess photocatalytic properties, which enable concrete to self-clean and promote environmental sustainability by breaking down SO_x and NO_x compounds present in the air. Additionally, it also possesses antimicrobial properties [140,141]. To explore its potential in modern construction, researchers have incorporated NT into printable concrete, where it has been shown to significantly enhance both functional and structural performance. Zahabizadeh et al. [142,143] demonstrated that NT surface coatings improve photocatalytic activity under light

exposure, with higher coating rates producing more uniform particle distribution and greater dye degradation efficiency. Specimens coated after seven days exhibited the highest efficiency due to favorable surface conditions, while extended curing led to reduced adsorption capacity from pore refinement and densification.

Beyond surface coatings, incorporating NT directly into printable mixes improves both buildability and functional performance. Rheologically, NT increases static yield stress while reducing dynamic yield stress and plastic viscosity, producing pastes that extrude smoothly yet retain stability after deposition. At an optimum dosage of around 3% with a w/c of 0.36, buildability improved markedly, up to 3.24 times the reference mix, supporting more than 120 layers without collapse. Functionally, NT enhances photocatalytic self-cleaning, as shown in Figure 19. Under UV irradiation, NT-containing specimens exhibited substantially higher colour degradation rates than controls, with photocatalytic removal of Rhodamine B dye exceeding 230–280% of the reference over 6h. Since greater colour change directly reflects stronger photocatalytic activity, this behaviour confirms NT's ability to impart durable self-cleaning properties. Together, these findings establish NT as a multifunctional additive that not only enhances rheology and buildability but also promotes sustainability in 3DPC through photocatalytic depollution and reduced maintenance demands [144].

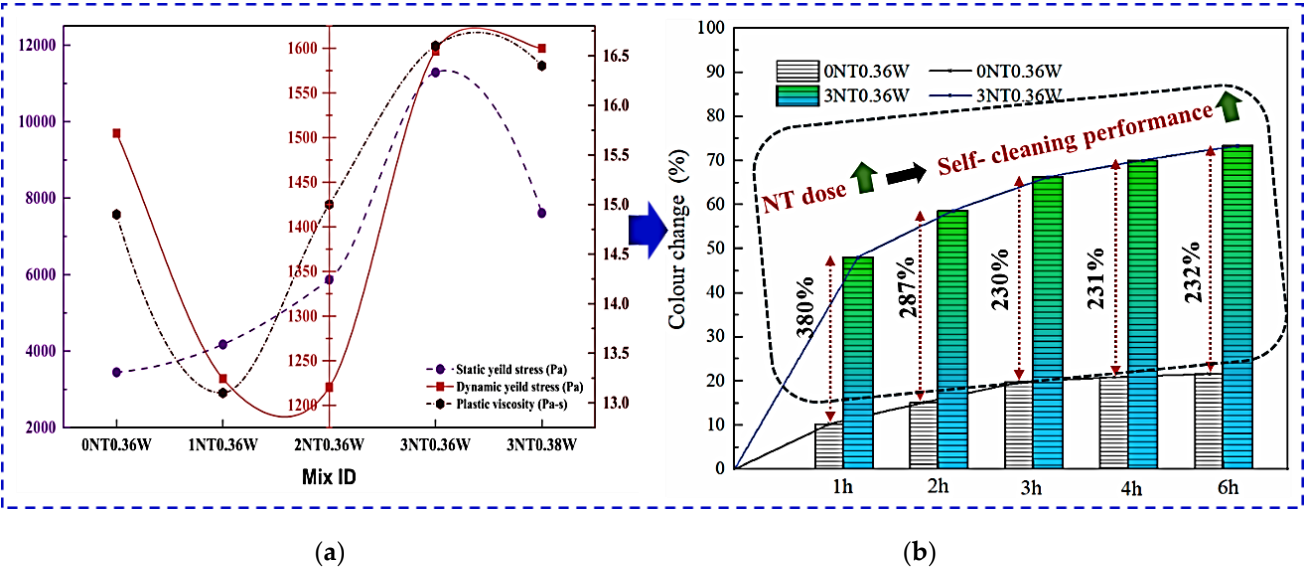


Figure 19. Influence of NT incorporation on 3DPC: (a) Rheological behaviour; (b) Photocatalytic self-cleaning performance. Modified from [143].

NT coatings also modify surface topography by filling irregularities and exposing hydration by-products such as C-S-H and Ca(OH)_2 , thereby enhancing overall structural integrity [46]. These findings highlight the potential of NT to advance the functional and structural performance of 3D-printed cementitious materials, though optimizing dosage and application methods remains critical.

In summary, the literature reviewed so far consistently indicates that the inclusion of NMs into printable concrete can significantly influence its properties in both fresh and hardened states. Table 1 below provides a summary of additional research investigating the effects of incorporating NMs into printable concrete and their interactions with other materials.

Table 1. Additional studies on NMs in 3DPC: dosages, additives, and their reported effects.

S.No	Nano material	Additional materials	Dosage of NMs (% of mass of cement/ binder)	Inferences	References
1	Graphene	-	0.5-2	Pore-filling clustering at higher dosages leads to an improvement in tensile strength. Enhancement of mechanical strength and microstructure upon the addition of silica fume.	[145]
2	Titanium dioxide	Polypropylene (PP) fibres	0-0.03	Increased static yield stress, lower dynamic yield stress, and hydration acceleration. Void filling improved density and mechanical strength while reducing porosity by over 40%.	[144]
3	Calcium carbonate	–	0-3	Lower compressive strength in 3D-printed cement pastes, particularly along the printing direction, is attributed to higher porosity and a weaker ITZ. Early age strength gain occurs due to the filler effect and an accelerated hydration reaction, resulting in reduced anisotropy.	[146]
4	Calcium carbonate	Modified PP fiber	0-4	Improves buildability, shape stability, and mechanical strength; reduces flowability and setting time; increases density via surface area and filling effect. Higher dose caused particle agglomeration, reducing efficiency. Modified PP fibers provided skeletal support.	[147]

5	Silica	-	0-2	<p>Flexural and compressive strengths at an early age were enhanced due to accelerated hydration and pore filling.</p> <p>The excessive addition of NS caused agglomeration, which may have a negative impact on extrudability and printability.</p> <p>Improved interfacial transition zone and dense microstructure.</p>	[148]
6	Silica	-	0-1	<p>Improvements in rheological properties, thickening of mixes, reduction of setting time, enhancement of buildability and negative impact on pumpability.</p> <p>Densification of the microstructure increases the risk of carbonation at higher dosages.</p>	[117]
7	Silica	PP fibers	0-1	<p>NS enhanced the hydrophilicity of PP fibers, that improved cement bonding and mortar packing, led to smoother printability</p> <p>Double doped mix enhanced buildability around 1.25 times.</p> <p>Combined of NS and PP reduced anisotropy. Limited availability of water may reduce NS nucleation, which has a negative impact on compressive strength.</p>	[149]
8	Clay	-	0.4%	<p>Declination of Pumpability, higher shape retention, buildability and thixotropy.</p> <p>Enhancement of mechanical strength.</p>	[150]
9	Clay	-	0.5- 4	<p>Enhancements in rheological properties include a static yield stress</p>	[151]

				<p>improvement of up to 15 times and a near doubling of viscosity, as well as improvements in shape stability and buildability.</p> <p>The acceleration phase has resulted in increased heat, leading to accelerated C-S-H growth and nucleation, as well as improved matrix stiffening.</p>	
10	Clay	Carbohydrate complex chemical-based admixture	0-0.6	<p>Increased static yield stress and dynamic yield stress, reduced viscosity, and enhanced elasticity were observed, while VMA effects were minor, except at higher attapulgite doses.</p> <p>Lower static yield stress led to collapse or mixed elastic-plastic failures.</p>	[152]
11	Clay	Fly ash	Montmorillonite 0-1 Sepiolite 0-1	<p>Enhanced thixotropy, dynamic yield stress, shape retention, and buildability result in a stiff mix at a higher dosage.</p> <p>Fly ash improves thixotropy and structural build-up but slightly reduces recovery and natural tendencies.</p>	[153]
12	Clay	Gypsum	0-0.4	<p>Enlarged thixotropic area. Enhanced early and overall strength through nucleation, accelerated C-S-H formation, and reduced porosity.</p> <p>Combined materials led to a reduction in flowability, early hydration, refinement of pore structure, optimised rheological behaviour, and volume instability.</p>	[154]
13	Clay	Fly ash	0.5-2.5	<p>Reduced slump, elevated yield stresses, and increased plastic viscosity.</p>	[155]

				NC increased air entrainment because the fine particles absorb lubricated water. Trapping air led to a reduction in compressive strength and stiffness. Fly ash decreased slump and compressive strength at later ages while enhancing hydration, improving microstructure, and reducing induced bleeding through better particle packing and dispersion.	
--	--	--	--	---	--

Figure 20 demonstrates enhanced rheological behaviour, with increases in yield stress, thixotropy, and buildability, although workability tends to decline due to the high surface area of these particles. It also illustrates the variation of static yield stress (SYS) and dynamic yield stress (DYS) across different NMs, where the values plotted correspond to their optimum dosages by mass of binder. Negative values represent a reduction in the respective property, while zero indicates no available data. On the mechanical side (Figure 21), most NMs significantly increase compressive strength, reflecting their role in densifying the matrix and accelerating hydration. Flexural strength is also improved, though the extent varies with type and dosage. Unlike other nanoparticles, MWCNTs show limited benefits in strength development, despite their crack-bridging potential. Interestingly, NCa exhibits comparatively higher gains in flexural strength than one-dimensional NMs, though further investigation is needed to validate these findings.

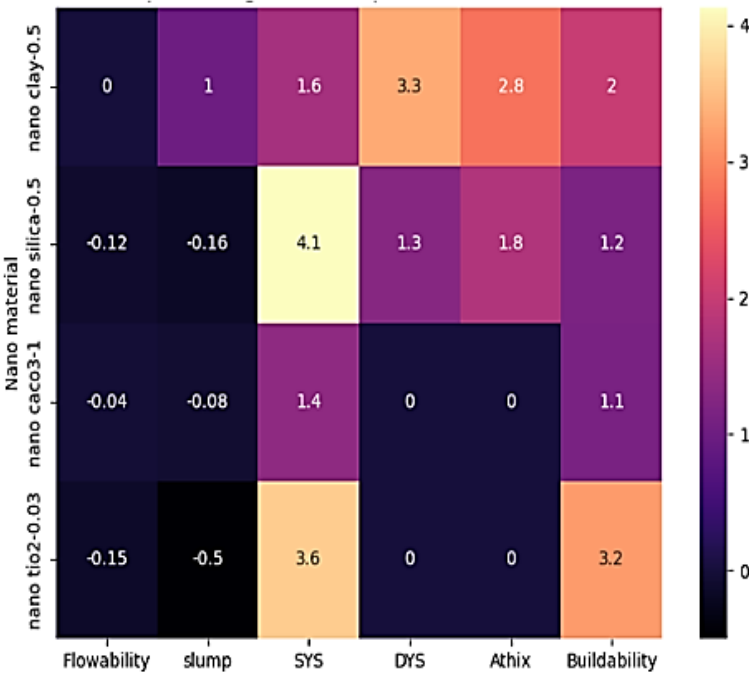


Figure 20. Modification of rheological properties with the addition of NMs in the printable mixes.

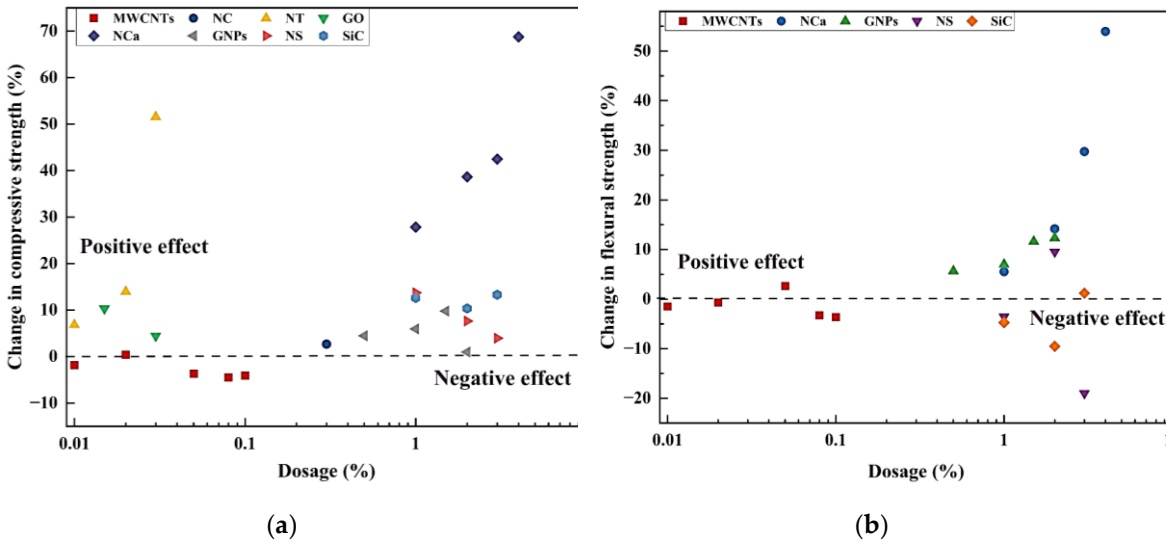


Figure 21. Variation of compressive strength (a) and flexural strength (b) with the addition of different nanoparticles.

5. Performance of NMs in Development of Sustainable 3DPC

5.1. Sustainability in 3DPC

Concrete is the second most widely used material in the world and contributes significantly to environmental burdens, mainly due to cement production. Cement was responsible for ~8% of global CO₂ emissions [156], with 40–60% linked to clinker production through combustion and calcination [157]. With demand expected to double by 2050 [158], assessing sustainability is essential.

Life Cycle Assessment (LCA) provides a structured approach to quantify impacts from raw material extraction to end-of-life. In 3DPC, LCA encompasses material production, construction, service life, and disposal, with a focus on CO₂ emissions and energy use. As illustrated in Figure 22, the framework highlights the optimisation of material use, reduction of carbon footprint, and energy savings as primary goals of sustainable 3DPC [159–161].

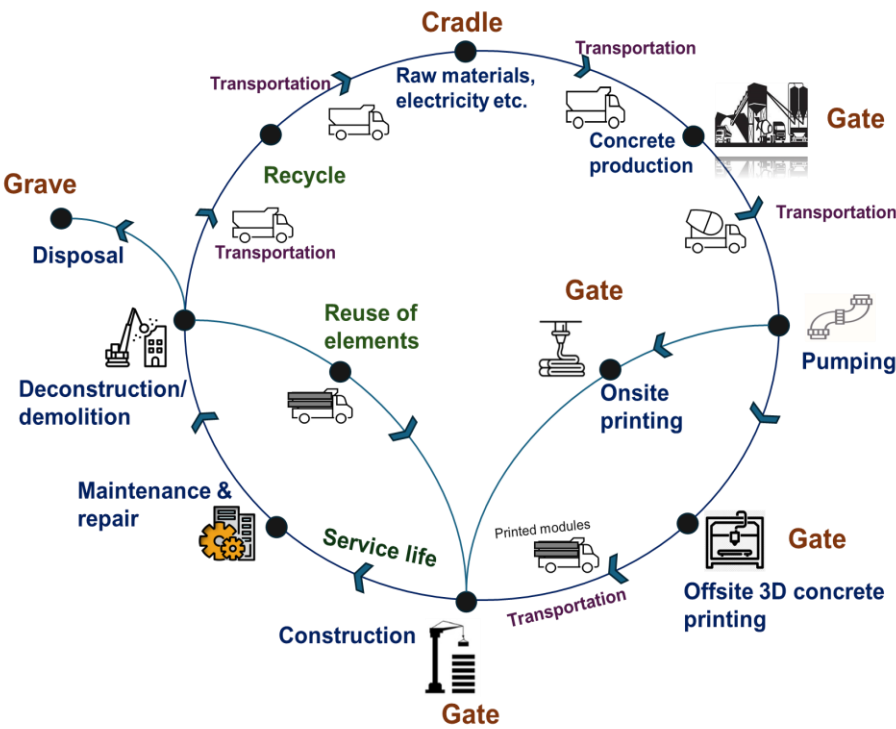


Figure 22. A schematic illustration of LCA of a 3D printed structure, emphasising the various gates within the LCA framework. Modified from [162].

5.2. Sustainability Challenges and Economic Implications of Nanomaterial Incorporation in 3DPC

The incorporation of NMs into Printable cementitious systems offer clear performance advantages, enhancing rheology, mechanical properties, and microstructural refinement at optimal dosages. These improvements result in reduced material use and extended service life. However, their adoption raises critical environmental and economic challenges that must be carefully assessed to establish net sustainability.

As shown in Figure 23, NM synthesis is an energy-intensive process and is often associated with elevated greenhouse gas emissions. For example, the production of cellulose nanofibres and cellulose nanocrystals requires 0.5–2.3 kWh/kg [163]. whereas GO demands 5,750–19,027 kWh/kg, with associated emissions of $1.06 \times e3$ – $2.36 \times e3$ kg CO₂-eq/kg depending on synthesis route [164]. Similarly, NT production through the sulfate process consumes between 8.8–11.1 kWh/kg and emits approximately 5 kg CO₂/kg, whereas the chloride process is more energy-efficient, consuming approximately 5.27 kWh/kg and emitting 4 kg CO₂/kg. The chloride process also offers advantages in terms of better particle size control and purity [165]. MWCNTs are even more demanding: ~261 kWh/kg for floating catalyst chemical vapour deposition, plus ~319 kWh for ultrasonication to disperse 2 kg of material [166]. As illustrated in Figure 23, full symbols represent nanoparticles synthesised using physical methods. In contrast, hollow symbols correspond to chemical processes, highlighting not only the overall energy and emission intensities but also the wide variations both across and within synthesis routes. These wide variations underscore the importance of synthesis method choice, as highlighted in Table 2, which summarises common routes and typical NMs produced.

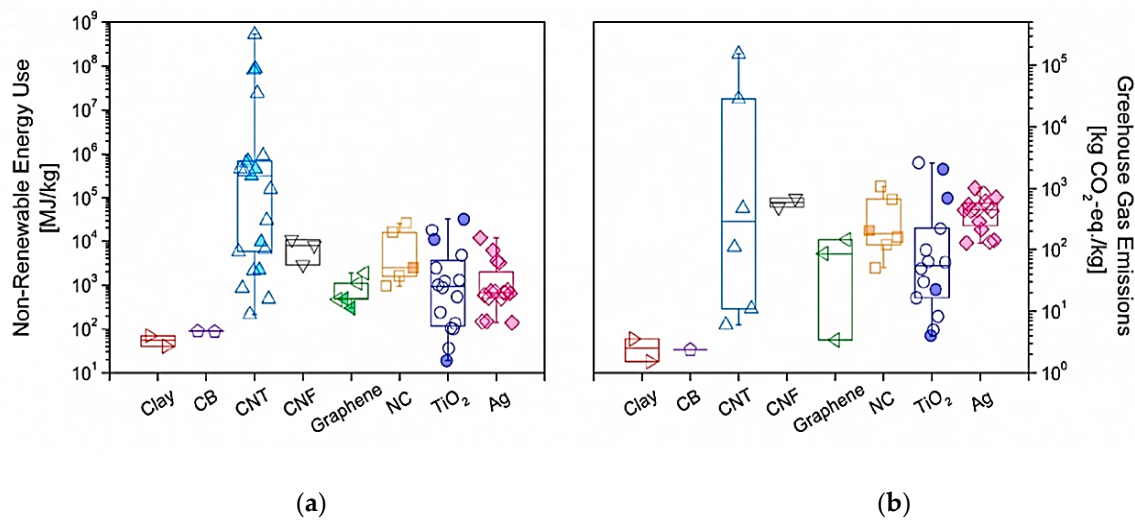


Figure 23. (a) Non-renewable energy usage and (b) Greenhouse gas emissions for various types of NMs [167].

Table 2. Common synthesis methods.

Synthesis Method	Nanomaterials Commonly Produced
Sol-Gel	SiO ₂ , TiO ₂ , ZrO ₂ , Fe ₂ O ₃ , other metal oxide nanoparticles
Hydrothermal	SiO ₂ , TiO ₂ , Fe ₃ O ₄ , ZrO ₂ , nano clays (montmorillonite, attapulgite), other oxides

Co-precipitation	Fe ₃ O ₄ , ZrO ₂ , other metal oxide nanoparticles
Green Synthesis	SiO ₂ , TiO ₂ , Fe ₂ O ₃ , ZrO ₂ , Fe ₃ O ₄ (using plant extracts, etc.)
CVD	CNTs, graphene, other carbon nanomaterials
Arc Discharge	CNTs, fullerenes, carbon onions
Laser Ablation	CNTs, fullerenes, graphene, metal nanoparticles
Electrochemical Exfoliation	Graphene, graphene oxide
Mechanical/ Ultrasonic Exfoliation	Graphene, nano clays (montmorillonite, attapulgite)
Solution/ Melt Blending, In-situ Polymerisation	Montmorillonite and attapulgite nano clay composites

Despite these costs, NMs can deliver substantial structural benefits. For instance, incorporating 0.2% MWCNTs can increase flexural strength by up to 269%, enabling a 48% reduction in material thickness while maintaining equivalent performance. This structural optimisation translates to a net energy saving of ~97 kWh in highway construction applications [166]. Such duality illustrates the central dilemma: while synthesis imposes significant energy and emission burdens, enhanced material efficiency and durability may partly offset these impacts. Translating performance into sustainability metrics, however, is not a straightforward process. Studies emphasise the difficulty of aligning mechanical data with LCA outcomes, due to inconsistent characterisation techniques and limited commercial transparency. Accurate integration of durability and performance metrics into LCA frameworks remains essential to ensure reliability.

From an economic perspective, NMs substantially increase the cost of 3DPC. Batikha et al. [4] reported that conventional structural concrete with a strength of about 40 MPa costs around USD 68 per cubic metre, whereas 3DPC already reaches about USD 259 per cubic metre due to binder-rich mixes and specialised admixtures. The addition of NMs raises this cost further; for example, incorporating 0.2% MWCNTs increases the price by approximately USD 675 per cubic metre, which is nearly ten times that of conventional concrete. Although these additions provide clear performance benefits such as improved durability, self-cleaning ability, and pollutant degradation, the high material costs remain a significant barrier to scalability.

Table 3. Estimated additional cost per m³ of 3DPC with various NMs (Data provided by Ad-Nano Technologies Pvt. Ltd., India).

Sl. No	Nanomaterial	Purity (%)	Size (nm)	~Surface area (m ² /g)	Approximate price Per kg (USD)	Dosage considered (% by binder mass)	Mass of NMs per m ³ (kg)	Additional cost per m ³ (USD)
1	Montmorillonite	~99.9	<500	180-220	58.61	0.5	4.5	263.75
2	Silicon Dioxide	>99.9	<100	120	57.44	0.5	4.5	258.48
3	Graphene oxide	~99	0.8-2 (thickness) D50-10µm	120	339.95	0.03	0.27	91.79
4	Titanium Dioxide	>99.9	<100	150	57.44	0.75	6.75	387.72
5	Multiwalled carbon nanotubes	~99%	10-20 (diameter), ~10µm (length)	230	375.12	0.2	1.8	675.216

Therefore, to move forward, future LCA models must incorporate performance metrics, standardise functional units, and include robust uncertainty analysis. Only then can the construction industry make informed decisions about balancing performance gains with environmental and economic sustainability, paving the way for more responsible and scalable integration of NMs. Notably, while NMs address sustainability challenges at the material scale, their long-term impact also depends on how these materials are deployed within structural systems. This highlights the role of structural optimisation as a complementary strategy for sustainable 3D printing and construction.

5.3. Role of Structural Optimisation for Sustainability

The synergistic integration of material optimisation and topology optimisation holds significant potential for sustainable and efficient construction [168], as both approaches are inherently interdependent and enable reductions in material consumption while maintaining structural performance, as illustrated in Figure 24. Recent studies [169,170] emphasised that additive construction methods can significantly reduce material usage through topology optimisation, achieve complex geometries without auxiliary supports, and highlight the importance of incorporating sustainability evaluation frameworks such as LCA to ensure that these advances translate into genuinely sustainable 3D-printed structures.

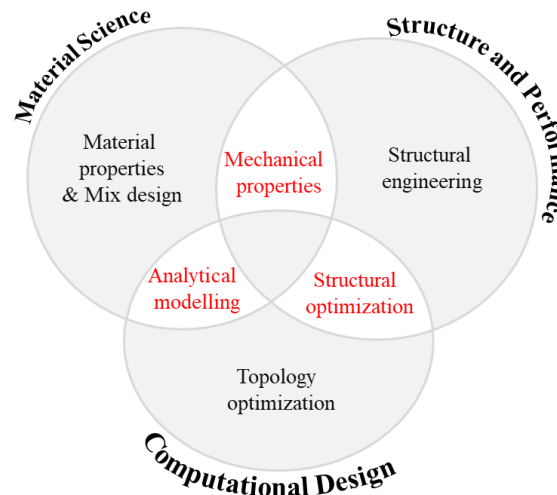


Figure 24. Framework illustrating interdependencies between research areas in 3DPC. Modified from [171].

Utilising advanced computational tools, such as topology enhancement, finite element analysis, generative and parametric design, and real-time feedback systems, can enhance the effectiveness, performance, and sustainability of 3DPC projects. Innovative methods combine structural optimisation with form-finding design, enabling unique expressions and improving resource efficiency in architecture. Additive construction techniques can reduce material usage through optimisation, resulting in sustainable benefits. Optimised non-standard geometries can save material and reduce weight in load-bearing applications. High-performance concrete is vital for complex structures made using digital fabrication methods. Combining high-performance concrete with structural optimisation can significantly reduce the environmental impact of digitally fabricated concrete structures [169,172–176].

De Schutter et al. [2] noted that the environmental impact of 3D printing with concrete is influenced by the complexity of the structure's shape. Structural optimisation and functional hybridisation design strategies enable the use of materials only where they are needed structurally or functionally. This optimisation increases the complexity of the shape and reduces material usage in digitally fabricated concrete. Consequently, digitally fabricated concrete is expected to outperform conventionally produced concrete structures in terms of environmental performance over their service life for structures with similar functionality. In 3D printed concrete, controlling rheology using techniques such as active rheology control and active stiffening control is crucial for achieving proper flow and solidification, which supports subsequent layers. The layered structure of 3D printing yields anisotropic mechanical properties, necessitating the development of new design models and testing methods to account for these properties. Material optimisation, considering both cement type and aggregate, is essential for creating high-performance printable materials. Design codes need revision to account for anisotropic behaviour accurately. Despite being early in development, 3DPC offers environmental benefits through waste reduction and cost-effectiveness in construction.

6. Conclusions

This review consolidates current insights into the role of NMs in 3DPC, highlighting their influence from fresh-state rheology to hardened performance, microstructural development, and eco-functionality. The key conclusions drawn from the critical analysis are as follows:

- I. Most of the NMs significantly enhance the rheological properties of the printable concrete when used in a limited dosage. Specifically, NMs such as NC (0.5%), NS (0.5%), NCa (1%), and NT (0.03%) have been shown to enhance the cohesiveness and yield stress of the mix, thereby improving shape retention and buildability post-extrusion. Notably, the addition of NS resulted

in a substantial increase of approximately 410% in static yield stress, followed by a 360% improvement.

- II. At optimal dosages, NMs reduced flowability by 10–15% and slump by up to 50%. This reduction is attributed to their high surface area and particle reactivity, which increase water demand and thicken the mix. Consequently, higher superplasticiser dosages are required to restore workability. The stiffening effect impairs pumpability and extrusion, underscoring a trade-off between buildability and fresh-state performance.
- III. NC enhances green strength and early stiffness through its flocculation-promoting capacity, acting as a viscosity-modifying agent, while NS accelerates hydration kinetics and improves structural buildup and shape retention. An excessive dosage of NMs leads to agglomeration and pumpability issues, often resulting in unprintable mixes. Almost all NMs have a negative impact on the flowability of the blend due to their larger surface area.
- IV. The addition of NMs into 3D printable concrete significantly enhances mechanical performance, with optimal dosages (~0.05–1.0 wt.%) yielding up to a 70% improvement in compressive strength and a 55% improvement in flexural strength. NMs like GO and GNPs offer high efficiency at low dosages (~0.1–1 wt.%), while mineral-based NMs (NS, NCa) provide moderate, consistent improvements between ~20 to 35%. This enhancement is attributed to improved nucleation, densification of the matrix, and effective stress transfer. Beyond optimal dosage, the disruption of agglomeration and hydration kinetics degrades performance. Thus, NM selection and dosage tuning are critical to maximising reinforcement efficiency in printable cementitious systems.
- V. Incorporating NMs improves mechanical properties of concrete through microstructural densification, pore filling, and accelerated cement hydration. Few carbon-based NMs form crack-bridging networks that enhance interlayer bonding and reduce anisotropy. However, anisotropic weaknesses persist in specific configurations due to uneven material distribution and weak interlayer bonding, necessitating further studies.
- VI. NMs can be embedded into printable concrete to impart unique functionalities. For instance, adding NT enables concrete to clean itself by breaking down over 70% of surface pollutants within 6 hours of exposure to light, while GNPs enhance its self-sensing ability.
- VII. Dispersion of NMs is a significant challenge. Improper dispersion leads to agglomeration, which negatively impacts both rheological and mechanical properties. Techniques such as ultrasonication can improve uniform distribution, but they also increase production costs and energy demands. Enhanced strategies for effective NM incorporation are needed to minimise these drawbacks.
- VIII. The synergistic use of NMs with SCMs and fibres provide enhanced fresh and hardened properties; in combination with superplasticisers, this reduces water demand. However, excessive fibre dosages lead to blockages and inefficient printing.
- IX. Although NMs improve concrete properties, their production is energy-intensive, resulting in high environmental footprints. Topology optimisation techniques can further enhance sustainability by minimising material usage without compromising structural integrity in 3DPC.

7. Knowledge Gaps in NM-Modified 3DPC

The use of NMs in 3DPC represents a significant step in digital construction; however, several scientific and engineering challenges remain unresolved. A fundamental gap lies in the limited understanding of the multiscale relationships between the physicochemical characteristics of NMs, fresh-state rheology, and early-age structural development. Determining the appropriate dosage remains uncertain, as overdosing can lead to agglomeration, uncontrolled thixotropy, and unstable yield stress, all of which directly compromise printability and interlayer bonding.

Although mix design strategies have advanced, anisotropy at the interfaces between printed layers remains a significant limitation. This issue is aggravated by non-uniform nanomaterial distribution and weak interfacial bonding. Dispersion techniques, such as ultrasonic and high-shear

mixing, have improved performance at the laboratory scale; however, achieving uniform reinforcement in large-scale applications remains challenging.

From a design perspective, topology optimisation is rarely applied even though it offers clear potential to reduce structural dead weight and improve efficiency. Current approaches do not adequately incorporate NM-specific mechanical and durability data into computational models. On the sustainability side, existing life cycle assessment frameworks are too generalised to capture the embodied energy and environmental footprint of nanomaterial production, the benefits of extended service life, or the complexities of end-of-life recycling.

Standardisation also represents a significant shortcoming. Established protocols such as ASTM C1437, EN 196-1, and ASTM C109 were not designed for printable mortars and fail to measure critical parameters such as buildability, open time, interlayer bond strength, and directional mechanical properties. Furthermore, international design codes, including Eurocode 2 and ACI 318, have yet to adapt to the requirements of digitally fabricated and nanomaterial-modified concretes.

Therefore, these unresolved challenges highlight the need for targeted research that links material behaviour to process control, structural design, and sustainability evaluation, forming the basis for future research directions.

8. Future Research Directions

While NMs have demonstrated promising potential in enhancing the performance and functionality of 3DPC, several knowledge gaps and practical challenges remain unresolved. To advance research and enable large-scale, sustainable adoption, the following future research directions are proposed:

- I. Develop predictive multiscale frameworks that integrate NM dispersion dynamics, hydration kinetics, and rheological evolution with process parameters (e.g., extrusion rate, interlayer time, build height). Such models must be supported by scalable dispersion methods (high-shear, ultrasonic, and surface functionalisation) to ensure uniform distribution and reliable structural build-up.
- II. Incorporate NM-specific mechanical and durability datasets into structural design by embedding mechanical and durability properties into topology optimisation and anisotropy-aware computational models, enabling lightweight, resource-efficient, and performance-driven 3D printed structures.
- III. Advance sustainability assessments through refined LCA frameworks that capture service-life extension due to NM integration, and end-of-life recovery pathways such as recycling or carbonation.
- IV. Formulate dedicated test protocols for 3DPC that measure buildability, open time, interlayer adhesion, and anisotropic properties, addressing the limitations of current cement-based standards.
- V. Evolve design codes and guidelines toward performance-based criteria that explicitly account for digital fabrication processes, unconventional reinforcement layouts, and the durability enhancements achieved through NM integration.

Author Contributions: Conceptualization, S.J., M.T.L., K.S.K.K.R, B.K. and R.A.; methodology, J.S., M.T.L., K.S.K.K.R, B.K. and R.A.; formal analysis, S.J., M.T.L.; writing—original draft preparation, S.J.; writing—review and editing, M.T.L., K.S.K.K.R, B.K. and R.A. ; visualisation, S.J.; supervision, K.S.K.K.R, B.K. and R.A.; project administration, B.K. and R.A. All authors have read and agreed to the published version of the manuscript.

Funding: This research received no external funding.

Data Availability Statement: Not applicable.

Conflicts of Interest: The authors declare no conflicts of interest.

Abbreviations

The following abbreviations are used in this manuscript:

3DPC	Three-Dimensional Printing Concrete
AMC	Additive Manufacturing Concrete
C-S-H	Calcium Silicate Hydrate
CNT	Carbon Nanotube
GGBS	Ground Granulated Blast Furnace Slag
GNPs	Graphene Nanoparticles
GO	Graphene Oxide
LCA	Life Cycle Assessment
MWCNTs	Multiwalled Carbon Nanotubes
NASA	National Aeronautics and Space Administration
NC	Nano Clay
NCa	Nano Calcium Carbonate
NMs	Nanomaterials
NS	Nano Silica
NT	Nano Titanium-dioxide
SDGs	Sustainable Development Goals
SCMs	Supplementary Cementitious Materials
VMA	Viscosity Modifying Agent

References

1. S. Lim, R.A. Buswell, T.T. Le, S.A. Austin, A.G.F. Gibb, T. Thorpe, Developments in construction-scale additive manufacturing processes, *Automation in Construction* 21 (2012) 262–268. <https://doi.org/10.1016/j.autcon.2011.06.010>.
2. G. De Schutter, K. Lesage, V. Mechtcherine, V.N. Nerella, G. Habert, I. Agusti-Juan, Vision of 3D printing with concrete – Technical, economic and environmental potentials, *Cement and Concrete Research* 112 (2018) 25–36. <https://doi.org/10.1016/j.cemconres.2018.06.001>.
3. S.A. Khan, M. Koç, S.G. Al-Ghamdi, Sustainability assessment, potentials and challenges of 3D printed concrete structures: A systematic review for built environmental applications, *Journal of Cleaner Production* 303 (2021) 127027. <https://doi.org/10.1016/j.jclepro.2021.127027>.
4. M. Batikha, R. Jotangia, M.Y. Baaj, I. Mousleh, 3D concrete printing for sustainable and economical construction: A comparative study, *Automation in Construction* 134 (2022) 104087. <https://doi.org/10.1016/j.autcon.2021.104087>.
5. J. Wang, Z. Liu, J. Hou, M. Ge, Research Progress and Trend Analysis of Concrete 3D Printing Technology Based on CiteSpace, *Buildings* 14 (2024) 989. <https://doi.org/10.3390/buildings14040989>.
6. T. Rayna, L. Striukova, From rapid prototyping to home fabrication: How 3D printing is changing business model innovation, *Technological Forecasting and Social Change* 102 (2016) 214–224. <https://doi.org/10.1016/j.techfore.2015.07.023>.
7. S. Al-Qutaifi, A. Nazari, A. Bagheri, Mechanical properties of layered geopolymer structures applicable in concrete 3D-printing, *Construction and Building Materials* 176 (2018) 690–699. <https://doi.org/10.1016/j.conbuildmat.2018.04.195>.
8. B. Panda, S.C. Paul, N.A.N. Mohamed, Y.W.D. Tay, M.J. Tan, Measurement of tensile bond strength of 3D printed geopolymer mortar, *Measurement* 113 (2018) 108–116. <https://doi.org/10.1016/j.measurement.2017.08.051>.
9. C. Gosselin, R. Duballet, Ph. Roux, N. Gaudillière, J. Dirrenberger, Ph. Morel, Large-scale 3D printing of ultra-high performance concrete – a new processing route for architects and builders, *Materials & Design* 100 (2016) 102–109. <https://doi.org/10.1016/j.matdes.2016.03.097>.
10. T. Marchment, J.G. Sanjayan, B. Nematollahi, M. Xia, Interlayer Strength of 3D Printed Concrete, in: *3D Concrete Printing Technology*, Elsevier, 2019: pp. 241–264. <https://doi.org/10.1016/B978-0-12-815481-6.00012-9>.

11. S.C. Paul, G.P.A.G. van Zijl, M.J. Tan, I. Gibson, A review of 3D concrete printing systems and materials properties: current status and future research prospects, *Rapid Prototyping Journal* 24 (2018) 784–798. <https://doi.org/10.1108/RPJ-09-2016-0154>.
12. B. Nematollahi, M. Xia, J. Sanjayan, Current Progress of 3D Concrete Printing Technologies, in: Taipei, Taiwan, 2017. <https://doi.org/10.22260/ISARC2017/0035>.
13. B. Khoshnevis, S. Bukkapatnam, H. Kwon, J. Saito, Experimental investigation of contour crafting using ceramics materials, *Rapid Prototyping Journal* 7 (2001) 32–42. <https://doi.org/10.1108/13552540110365144>.
14. M. Xia, B. Nematollahi, J.G. Sanjayan, Development of Powder-Based 3D Concrete Printing Using Geopolymers, in: *3D Concrete Printing Technology*, Elsevier, 2019: pp. 223–240. <https://doi.org/10.1016/B978-0-12-815481-6.00011-7>.
15. A. Motalebi, M.A.H. Khondoker, G. Kabir, A systematic review of life cycle assessments of 3D concrete printing, *Sustainable Operations and Computers* 5 (2024) 41–50. <https://doi.org/10.1016/j.susoc.2023.08.003>.
16. 3D Printing In Construction Market Report, 2022-2027, (n.d.). <https://www.industryarc.com/Report/18132/3d-printing-in-construction-market.html> (accessed June 5, 2024).
17. NASA Looks to Advance 3D Printing Construction Systems for the Moon and Mars - NASA, (n.d.). <https://www.nasa.gov/technology/manufacturing-materials-3-d-printing/nasa-looks-to-advance-3d-printing-construction-systems-for-the-moon-and-mars/> (accessed June 5, 2024).
18. B. Zhu, B. Nematollahi, J. Pan, Y. Zhang, Z. Zhou, Y. Zhang, 3D concrete printing of permanent formwork for concrete column construction, *Cement and Concrete Composites* 121 (2021) 104039. <https://doi.org/10.1016/j.cemconcomp.2021.104039>.
19. J. Zhang, J. Wang, S. Dong, X. Yu, B. Han, A review of the current progress and application of 3D printed concrete, *Composites Part A: Applied Science and Manufacturing* 125 (2019) 105533. <https://doi.org/10.1016/j.compositesa.2019.105533>.
20. G.H. Ahmed, A review of “3D concrete printing”: Materials and process characterization, economic considerations and environmental sustainability, *Journal of Building Engineering* 66 (2023) 105863. <https://doi.org/10.1016/j.job.2023.105863>.
21. Y. Liu, L. Wang, Q. Yuan, J. Peng, Effect of coarse aggregate on printability and mechanical properties of 3D printed concrete, *Construction and Building Materials* 405 (2023) 133338. <https://doi.org/10.1016/j.conbuildmat.2023.133338>.
22. A.U. Rehman, J.-H. Kim, 3D Concrete Printing: A Systematic Review of Rheology, Mix Designs, Mechanical, Microstructural, and Durability Characteristics, *Materials* 14 (2021) 3800. <https://doi.org/10.3390/ma14143800>.
23. W. Zhou, Y. Zhang, L. Ma, V.C. Li, Influence of printing parameters on 3D printing engineered cementitious composites (3DP-ECC), *Cement and Concrete Composites* 130 (2022) 104562. <https://doi.org/10.1016/j.cemconcomp.2022.104562>.
24. P.S. Ambily, S.K. Kaliyavaradhan, N. Rajendran, Top challenges to widespread 3D concrete printing (3DCP) adoption – A review, *European Journal of Environmental and Civil Engineering* 28 (2024) 300–328. <https://doi.org/10.1080/19648189.2023.2213294>.
25. Y. Yang, C. Wu, Z. Liu, H. Wang, Q. Ren, Mechanical anisotropy of ultra-high performance fibre-reinforced concrete for 3D printing, *Cement and Concrete Composites* 125 (2022) 104310. <https://doi.org/10.1016/j.cemconcomp.2021.104310>.
26. A.V. Rahul, M.K. Mohan, G. De Schutter, K. Van Tittelboom, 3D printable concrete with natural and recycled coarse aggregates: Rheological, mechanical and shrinkage behaviour, *Cement and Concrete Composites* 125 (2022) 104311. <https://doi.org/10.1016/j.cemconcomp.2021.104311>.
27. Y. Chen, Y. Zhang, B. Pang, Z. Liu, G. Liu, Extrusion-based 3D printing concrete with coarse aggregate: Printability and direction-dependent mechanical performance, *Construction and Building Materials* 296 (2021) 123624. <https://doi.org/10.1016/j.conbuildmat.2021.123624>.
28. A. Kazemian, X. Yuan, E. Cochran, B. Khoshnevis, Cementitious materials for construction-scale 3D printing: Laboratory testing of fresh printing mixture, *Construction and Building Materials* 145 (2017) 639–647. <https://doi.org/10.1016/j.conbuildmat.2017.04.015>.

29. H. Ogura, V. Nerella, V. Mechtcherine, Developing and Testing of Strain-Hardening Cement-Based Composites (SHCC) in the Context of 3D-Printing, *Materials* 11 (2018) 1375. <https://doi.org/10.3390/ma11081375>.
30. G.M. Moelich, J. Kruger, R. Combrinck, Plastic shrinkage cracking in 3D printed concrete, *Composites Part B: Engineering* 200 (2020) 108313. <https://doi.org/10.1016/j.compositesb.2020.108313>.
31. M. Hambach, D. Volkmer, Properties of 3D-printed fiber-reinforced Portland cement paste, *Cement and Concrete Composites* 79 (2017) 62–70. <https://doi.org/10.1016/j.cemconcomp.2017.02.001>.
32. A. Perrot, D. Rangeard, A. Pierre, Structural built-up of cement-based materials used for 3D-printing extrusion techniques, *Mater Struct* 49 (2016) 1213–1220. <https://doi.org/10.1617/s11527-015-0571-0>.
33. Y. Che, S. Tang, H. Yang, W. Li, M. Shi, Influences of Air-Voids on the Performance of 3D Printing Cementitious Materials, *Materials* 14 (2021) 4438. <https://doi.org/10.3390/ma14164438>.
34. K. Manikandan, K. Wi, X. Zhang, K. Wang, H. Qin, Characterizing cement mixtures for concrete 3D printing, *Manufacturing Letters* 24 (2020) 33–37. <https://doi.org/10.1016/j.mfglet.2020.03.002>.
35. H. Bayat, A. Kashani, Analysis of rheological properties and printability of a 3D-printing mortar containing silica fume, hydrated lime, and blast furnace slag, *Materials Today Communications* 37 (2023) 107128. <https://doi.org/10.1016/j.mtcomm.2023.107128>.
36. S. Muthukrishnan, H.W. Kua, L.N. Yu, J.K.H. Chung, Fresh Properties of Cementitious Materials Containing Rice Husk Ash for Construction 3D Printing, *J. Mater. Civ. Eng.* 32 (2020) 04020195. [https://doi.org/10.1061/\(ASCE\)MT.1943-5533.0003230](https://doi.org/10.1061/(ASCE)MT.1943-5533.0003230).
37. M. Pimentel Tinoco, L. Gouvêa, K. De Cássia Magalhães Martins, R. Dias Toledo Filho, O. Aurelio Mendoza Reales, The use of rice husk particles to adjust the rheological properties of 3D printable cementitious composites through water sorption, *Construction and Building Materials* 365 (2023) 130046. <https://doi.org/10.1016/j.conbuildmat.2022.130046>.
38. B. Panda, J.H. Lim, M.J. Tan, Mechanical properties and deformation behaviour of early age concrete in the context of digital construction, *Composites Part B: Engineering* 165 (2019) 563–571. <https://doi.org/10.1016/j.compositesb.2019.02.040>.
39. Z. Liu, M. Li, Y. Weng, T.N. Wong, M.J. Tan, Mixture Design Approach to optimize the rheological properties of the material used in 3D cementitious material printing, *Construction and Building Materials* 198 (2019) 245–255. <https://doi.org/10.1016/j.conbuildmat.2018.11.252>.
40. Y. Chen, S. Chaves Figueiredo, Z. Li, Z. Chang, K. Jansen, O. Çopuroğlu, E. Schlangen, Improving printability of limestone-calcined clay-based cementitious materials by using viscosity-modifying admixture, *Cement and Concrete Research* 132 (2020) 106040. <https://doi.org/10.1016/j.cemconres.2020.106040>.
41. Y. Chen, K. Jansen, H. Zhang, C. Romero Rodriguez, Y. Gan, O. Çopuroğlu, E. Schlangen, Effect of printing parameters on interlayer bond strength of 3D printed limestone-calcined clay-based cementitious materials: An experimental and numerical study, *Construction and Building Materials* 262 (2020) 120094. <https://doi.org/10.1016/j.conbuildmat.2020.120094>.
42. W.-J. Long, C. Lin, J.-L. Tao, T.-H. Ye, Y. Fang, Printability and particle packing of 3D-printable limestone calcined clay cement composites, *Construction and Building Materials* 282 (2021) 122647. <https://doi.org/10.1016/j.conbuildmat.2021.122647>.
43. P.R.K. Soda, A. Dwivedi, S. C M, S. Gupta, Development of 3D printable stabilized earth-based construction materials using excavated soil: Evaluation of fresh and hardened properties, *Science of The Total Environment* 924 (2024) 171654. <https://doi.org/10.1016/j.scitotenv.2024.171654>.
44. Effect of Nanoclay on the Printability of Extrusion-based 3D Printable Mortar, *NanoWorld J* 9 (2023). <https://doi.org/10.17756/nwj.2023-s2-010>.
45. O.A. Mendoza Reales, P. Duda, E.C.C.M. Silva, M.D.M. Paiva, R.D.T. Filho, Nanosilica particles as structural buildup agents for 3D printing with Portland cement pastes, *Construction and Building Materials* 219 (2019) 91–100. <https://doi.org/10.1016/j.conbuildmat.2019.05.174>.
46. P. De Matos, T. Zat, K. Corazza, E. Fensterseifer, R. Sakata, G. Mohamad, E. Rodríguez, Effect of TiO₂ Nanoparticles on the Fresh Performance of 3D-Printed Cementitious Materials, *Materials* 15 (2022) 3896. <https://doi.org/10.3390/ma15113896>.

47. J. Liu, P. Tran, T. Ginigaddara, P. Mendis, Exploration of using graphene oxide for strength enhancement of 3D-printed cementitious mortar, *Additive Manufacturing Letters* 7 (2023) 100157. <https://doi.org/10.1016/j.addlet.2023.100157>.
48. P. Sikora, M. Chougan, K. Cuevas, M. Liebscher, V. Mechtcherine, S.H. Ghaffar, M. Liard, D. Lootens, P. Krivenko, M. Sanytsky, D. Stephan, The effects of nano- and micro-sized additives on 3D printable cementitious and alkali-activated composites: a review, *Appl Nanosci* 12 (2022) 805–823. <https://doi.org/10.1007/s13204-021-01738-2>.
49. A.M. Onaizi, G.F. Huseien, N.H.A.S. Lim, M. Amran, M. Samadi, Effect of nanomaterials inclusion on sustainability of cement-based concretes: A comprehensive review, *Construction and Building Materials* 306 (2021) 124850. <https://doi.org/10.1016/j.conbuildmat.2021.124850>.
50. M. Razzaghian Ghadikolaee, E. Cerro-Prada, Z. Pan, A. Habibnejad Korayem, Nanomaterials as Promising Additives for High-Performance 3D-Printed Concrete: A Critical Review, *Nanomaterials* 13 (2023) 1440. <https://doi.org/10.3390/nano13091440>.
51. L.G. Li, Z.-Q. Fang, S.-H. Chu, A.K.H. Kwan, Improving mechanical properties of 3D printed mortar through synergistic effects of fly ash microspheres and nanosilica, *Magazine of Concrete Research* 77 (2025) 255–269. <https://doi.org/10.1680/jmacr.24.00244>.
52. P. Jin, M. Hasany, M. Kohestanian, M. Mehrali, Micro/nano additives in 3D printing concrete, *Cement and Concrete Composites* 155 (2025) 105799. <https://doi.org/10.1016/j.cemconcomp.2024.105799>.
53. H. Saleem, S.J. Zaidi, N.A. Alnuaimi, Recent Advancements in the Nanomaterial Application in Concrete and Its Ecological Impact, *Materials* 14 (2021) 6387. <https://doi.org/10.3390/ma14216387>.
54. Effect of Red Mud, Nanoclay, and Natural Fiber on Fresh and Rheological Properties of Three-Dimensional Concrete Printing, *MJ* 118 (2021). <https://doi.org/10.14359/51733108>.
55. Y. Zhang, Y. Zhang, G. Liu, Y. Yang, M. Wu, B. Pang, Fresh properties of a novel 3D printing concrete ink, *Construction and Building Materials* 174 (2018) 263–271. <https://doi.org/10.1016/j.conbuildmat.2018.04.115>.
56. S. Kaushik, M. Sonebi, G. Amato, A. Perrot, U.K. Das, Influence of nanoclay on the fresh and rheological behaviour of 3D printing mortar, *Materials Today: Proceedings* 58 (2022) 1063–1068. <https://doi.org/10.1016/j.matpr.2022.01.108>.
57. M.M. Ali, G. Nassrullah, R.K. Abu Al-Rub, B. El-Khasawneh, S.H. Ghaffar, T.-Y. Kim, Influence of carbon nanotubes on printing quality and mechanical properties of 3D printed cementitious materials, *Developments in the Built Environment* 18 (2024) 100415. <https://doi.org/10.1016/j.dibe.2024.100415>.
58. A.H. Alami, A.G. Olabi, M. Ayoub, H. Aljaghoub, S. Alasad, M.A. Abdelkareem, 3D Concrete Printing: Recent Progress, Applications, Challenges, and Role in Achieving Sustainable Development Goals, *Buildings* 13 (2023) 924. <https://doi.org/10.3390/buildings13040924>.
59. D.J.M. Flower, J.G. Sanjayan, Green house gas emissions due to concrete manufacture, *Int J Life Cycle Assess* 12 (2007) 282–288. <https://doi.org/10.1065/lca2007.05.327>.
60. R.J. Flatt, T. Wangler, On sustainability and digital fabrication with concrete, *Cement and Concrete Research* 158 (2022) 106837. <https://doi.org/10.1016/j.cemconres.2022.106837>.
61. M.P. Tinoco, É.M. De Mendonça, L.I.C. Fernandez, L.R. Caldas, O.A.M. Reales, R.D. Toledo Filho, Life cycle assessment (LCA) and environmental sustainability of cementitious materials for 3D concrete printing: A systematic literature review, *Journal of Building Engineering* 52 (2022) 104456. <https://doi.org/10.1016/j.jobbe.2022.104456>.
62. K. Heywood, P. Nicholas, Sustainability and 3D concrete printing: identifying a need for a more holistic approach to assessing environmental impacts, *ARIN* 2 (2023) 12. <https://doi.org/10.1007/s44223-023-00030-3>.
63. B. Panda, C. Unluer, M.J. Tan, Investigation of the rheology and strength of geopolymer mixtures for extrusion-based 3D printing, *Cement and Concrete Composites* 94 (2018) 307–314. <https://doi.org/10.1016/j.cemconcomp.2018.10.002>.
64. S. Mujeeb, M. Samudrala, B.A. Lanjewar, R. Chippagiri, M. Kamath, R.V. Ralegaonkar, Development of Alkali-Activated 3D Printable Concrete: A Review, *Energies* 16 (2023) 4181. <https://doi.org/10.3390/en16104181>.

65. S.A. Khan, S.M.U. Ghazi, H. Amjad, M. Imran, R.A. Khushnood, Emerging horizons in 3D printed cement-based materials with nanomaterial integration: A review, *Construction and Building Materials* 411 (2024) 134815. <https://doi.org/10.1016/j.conbuildmat.2023.134815>.
66. M. Razzaghian Ghadikolaee, E. Cerro-Prada, Z. Pan, A. Habibnejad Korayem, Nanomaterials as Promising Additives for High-Performance 3D-Printed Concrete: A Critical Review, *Nanomaterials* 13 (2023) 1440. <https://doi.org/10.3390/nano13091440>.
67. R.P. Feynman, There's plenty of room at the bottom, *Resonance* 16 (1999) 890–905.
68. S. Mehnath, A.K. Das, S.K. Verma, M. Jeyaraj, Biosynthesized/green-synthesized nanomaterials as potential vehicles for delivery of antibiotics/drugs, in: *Comprehensive Analytical Chemistry*, Elsevier, 2021: pp. 363–432. <https://doi.org/10.1016/bs.coac.2020.12.011>.
69. K. Sobolev, How Nanotechnology Can Change the Concrete World Part Two of a Two-Part Series, *American Ceramic Society Bulletin* 84 (2005).
70. N. Abid, A.M. Khan, S. Shujait, K. Chaudhary, M. Ikram, M. Imran, J. Haider, M. Khan, Q. Khan, M. Maqbool, Synthesis of nanomaterials using various top-down and bottom-up approaches, influencing factors, advantages, and disadvantages: A review, *Advances in Colloid and Interface Science* 300 (2022) 102597. <https://doi.org/10.1016/j.cis.2021.102597>.
71. N. Baig, I. Kammakakam, W. Falath, Nanomaterials: a review of synthesis methods, properties, recent progress, and challenges, *Mater. Adv.* 2 (2021) 1821–1871. <https://doi.org/10.1039/D0MA00807A>.
72. Mohajerani, Burnett, Smith, Kurmus, Milas, Arulrajah, Horpibulsuk, Abdul Kadir, Nanoparticles in Construction Materials and Other Applications, and Implications of Nanoparticle Use, *Materials* 12 (2019) 3052. <https://doi.org/10.3390/ma12193052>.
73. S.S. Regalla, S.K. N, Effect of nano SiO₂ on rheology, nucleation seeding, hydration mechanism, mechanical properties and microstructure amelioration of ultra-high-performance concrete, *Case Studies in Construction Materials* 20 (2024) e03147. <https://doi.org/10.1016/j.cscm.2024.e03147>.
74. T.J. Gutiérrez, A.G. Ponce, V.A. Alvarez, Nano-clays from natural and modified montmorillonite with and without added blueberry extract for active and intelligent food nanopackaging materials, *Materials Chemistry and Physics* 194 (2017) 283–292. <https://doi.org/10.1016/j.matchemphys.2017.03.052>.
75. B. Panda, S. Ruan, C. Unluer, M.J. Tan, Improving the 3D printability of high volume fly ash mixtures via the use of nano attapulgite clay, *Composites Part B: Engineering* 165 (2019) 75–83. <https://doi.org/10.1016/j.compositesb.2018.11.109>.
76. C.-Y. Hsu, Z.H. Mahmoud, S. Abdullaev, F.K. Ali, Y. Ali Naeem, R. Mzahir Mizher, M. Morad Karim, A.S. Abdulwahid, Z. Ahmadi, S. Habibzadeh, E. Kianfar, Nano titanium oxide (nano-TiO₂): A review of synthesis methods, properties, and applications, *Case Studies in Chemical and Environmental Engineering* 9 (2024) 100626. <https://doi.org/10.1016/j.csee.2024.100626>.
77. G. Land, D. Stephan, Controlling cement hydration with nanoparticles, *Cement and Concrete Composites* 57 (2015) 64–67. <https://doi.org/10.1016/j.cemconcomp.2014.12.003>.
78. M.A. Khan, M.K. Imam, K. Irshad, H.M. Ali, M.A. Hasan, S. Islam, Comparative Overview of the Performance of Cementitious and Non-Cementitious Nanomaterials in Mortar at Normal and Elevated Temperatures, *Nanomaterials* 11 (2021) 911. <https://doi.org/10.3390/nano11040911>.
79. A. Cuesta, A. Morales-Cantero, A.G. De La Torre, M.A.G. Aranda, Recent Advances in C-S-H Nucleation Seeding for Improving Cement Performances, *Materials* 16 (2023) 1462. <https://doi.org/10.3390/ma16041462>.
80. E. John, T. Matschei, D. Stephan, Nucleation seeding with calcium silicate hydrate – A review, *Cement and Concrete Research* 113 (2018) 74–85. <https://doi.org/10.1016/j.cemconres.2018.07.003>.
81. D. Kong, S. Huang, D. Corr, Y. Yang, S.P. Shah, Whether do nano-particles act as nucleation sites for C-S-H gel growth during cement hydration?, *Cement and Concrete Composites* 87 (2018) 98–109. <https://doi.org/10.1016/j.cemconcomp.2017.12.007>.
82. L.J. Jaramillo, R. Kalfat, Fresh and hardened performance of concrete enhanced with graphene nanoplatelets (GNPs), *Journal of Building Engineering* 75 (2023) 106945. <https://doi.org/10.1016/j.job.2023.106945>.

83. P. Zhang, D. Sha, Q. Li, S. Zhao, Y. Ling, Effect of Nano Silica Particles on Impact Resistance and Durability of Concrete Containing Coal Fly Ash, *Nanomaterials* 11 (2021) 1296. <https://doi.org/10.3390/nano11051296>.
84. C. Gu, Effect of Nano-TiO₂ on the Durability of Ultra-High Performance Concrete with and without a Flexural Load, *Ceramics - Silikaty* (2018) 374–381. <https://doi.org/10.13168/cs.2018.0033>.
85. H. Ma, Y. Li, C. Wang, Y. Li, X. Zhang, TiO₂-Based Photocatalysts for Removal of Low-Concentration NO_x Contamination, *Catalysts* 15 (2025) 103. <https://doi.org/10.3390/catal15020103>.
86. A. Mohammed, J.G. Sanjayan, W.H. Duan, A. Nazari, Graphene Oxide Impact on Hardened Cement Expressed in Enhanced Freeze–Thaw Resistance, *J. Mater. Civ. Eng.* 28 (2016) 04016072. [https://doi.org/10.1061/\(ASCE\)MT.1943-5533.0001586](https://doi.org/10.1061/(ASCE)MT.1943-5533.0001586).
87. M.T. Souza, I.M. Ferreira, E. Guzi De Moraes, L. Senff, A.P. Novaes De Oliveira, 3D printed concrete for large-scale buildings: An overview of rheology, printing parameters, chemical admixtures, reinforcements, and economic and environmental prospects, *Journal of Building Engineering* 32 (2020) 101833. <https://doi.org/10.1016/j.job.2020.101833>.
88. N. Roussel, Rheological requirements for printable concretes, *Cement and Concrete Research* 112 (2018) 76–85. <https://doi.org/10.1016/j.cemconres.2018.04.005>.
89. Q. Yuan, D. Zhou, K.H. Khayat, D. Feys, C. Shi, On the measurement of evolution of structural build-up of cement paste with time by static yield stress test vs. small amplitude oscillatory shear test, *Cement and Concrete Research* 99 (2017) 183–189. <https://doi.org/10.1016/j.cemconres.2017.05.014>.
90. Y.W.D. Tay, Y. Qian, M.J. Tan, Printability region for 3D concrete printing using slump and slump flow test, *Composites Part B: Engineering* 174 (2019) 106968. <https://doi.org/10.1016/j.compositesb.2019.106968>.
91. M. Rahman, S. Rawat, R. (Chunhui) Yang, A. Mahil, Y.X. Zhang, A comprehensive review on fresh and rheological properties of 3D printable cementitious composites, *Journal of Building Engineering* 91 (2024) 109719. <https://doi.org/10.1016/j.job.2024.109719>.
92. V.N. Nerella, M. Krause, V. Mechtcherine, Practice-Oriented Buildability Criteria for Developing 3D-Printable Concretes in the Context of Digital Construction, (2018). <https://doi.org/10.20944/preprints201808.0441.v1>.
93. B. Panda, Y.W.D. Tay, S.C. Paul, M.J. Tan, Current challenges and future potential of 3D concrete printing: Aktuelle Herausforderungen und Zukunftspotenziale des 3D-Druckens bei Beton, *Materialwissenschaft Werkst* 49 (2018) 666–673. <https://doi.org/10.1002/mawe.201700279>.
94. N. Roussel, G. Ovarlez, S. Garrault, C. Brumaud, The origins of thixotropy of fresh cement pastes, *Cement and Concrete Research* 42 (2012) 148–157. <https://doi.org/10.1016/j.cemconres.2011.09.004>.
95. S.K. Kaliyavaradhan, P.S. Ambily, P.R. Prem, S.B. Ghodke, Test methods for 3D printable concrete, *Automation in Construction* 142 (2022) 104529. <https://doi.org/10.1016/j.autcon.2022.104529>.
96. T.T. Le, S.A. Austin, S. Lim, R.A. Buswell, A.G.F. Gibb, T. Thorpe, Mix design and fresh properties for high-performance printing concrete, *Mater Struct* 45 (2012) 1221–1232. <https://doi.org/10.1617/s11527-012-9828-z>.
97. G. Ma, L. Wang, A critical review of preparation design and workability measurement of concrete material for largescale 3D printing, *Front. Struct. Civ. Eng.* 12 (2018) 382–400. <https://doi.org/10.1007/s11709-017-0430-x>.
98. V.N. Nerella, M. Näther, A. Iqbal, M. Butler, V. Mechtcherine, Inline quantification of extrudability of cementitious materials for digital construction, *Cement and Concrete Composites* 95 (2019) 260–270. <https://doi.org/10.1016/j.cemconcomp.2018.09.015>.
99. M.S. Choi, Y.J. Kim, J.K. Kim, Prediction of Concrete Pumping Using Various Rheological Models, *Int J Concr Struct Mater* 8 (2014) 269–278. <https://doi.org/10.1007/s40069-014-0084-1>.
100. S. Paritala, K.K. Singaram, I. Bathina, M.A. Khan, S.K.R. Jyosyula, Rheology and pumpability of mix suitable for extrusion-based concrete 3D printing – A review, *Construction and Building Materials* 402 (2023) 132962. <https://doi.org/10.1016/j.conbuildmat.2023.132962>.
101. C. Zhang, Z. Deng, C. Chen, Y. Zhang, V. Mechtcherine, Z. Sun, Predicting the static yield stress of 3D printable concrete based on flowability of paste and thickness of excess paste layer, *Cement and Concrete Composites* 129 (2022) 104494. <https://doi.org/10.1016/j.cemconcomp.2022.104494>.

102. J.H. Jo, B.W. Jo, W. Cho, J.-H. Kim, Development of a 3D Printer for Concrete Structures: Laboratory Testing of Cementitious Materials, *Int J Concr Struct Mater* 14 (2020) 13. <https://doi.org/10.1186/s40069-019-0388-2>.
103. K.-W. Lee, H.-J. Lee, M.-S. Choi, Correlation between thixotropic behavior and buildability for 3D concrete printing, *Construction and Building Materials* 347 (2022) 128498. <https://doi.org/10.1016/j.conbuildmat.2022.128498>.
104. J. Kruger, S. Cho, S. Zeranka, C. Viljoen, G. Van Zijl, 3D concrete printer parameter optimisation for high rate digital construction avoiding plastic collapse, *Composites Part B: Engineering* 183 (2020) 107660. <https://doi.org/10.1016/j.compositesb.2019.107660>.
105. A.V. Rahul, M. Santhanam, H. Meena, Z. Ghani, 3D printable concrete: Mixture design and test methods, *Cement and Concrete Composites* 97 (2019) 13–23. <https://doi.org/10.1016/j.cemconcomp.2018.12.014>.
106. J. Kruger, S. Zeranka, G. Van Zijl, 3D concrete printing: A lower bound analytical model for buildability performance quantification, *Automation in Construction* 106 (2019) 102904. <https://doi.org/10.1016/j.autcon.2019.102904>.
107. N. Roussel, A thixotropy model for fresh fluid concretes: Theory, validation and applications, *Cement and Concrete Research* 36 (2006) 1797–1806. <https://doi.org/10.1016/j.cemconres.2006.05.025>.
108. R. Jayathilakage, P. Rajeev, J.G. Sanjayan, Yield stress criteria to assess the buildability of 3D concrete printing, *Construction and Building Materials* 240 (2020) 117989. <https://doi.org/10.1016/j.conbuildmat.2019.117989>.
109. P. Ranjan Prem, D. Ravichandran, S. Kumar Kaliyavaradhan, P.S. Ambily, Comparative evaluation of rheological models for 3D printable concrete, *Materials Today: Proceedings* 65 (2022) 1594–1598. <https://doi.org/10.1016/j.matpr.2022.04.555>.
110. P. Feng, X. Meng, J.-F. Chen, L. Ye, Mechanical properties of structures 3D printed with cementitious powders, *Construction and Building Materials* 93 (2015) 486–497. <https://doi.org/10.1016/j.conbuildmat.2015.05.132>.
111. Y. Weng, M. Li, D. Zhang, M.J. Tan, S. Qian, Investigation of interlayer adhesion of 3D printable cementitious material from the aspect of printing process, *Cement and Concrete Research* 143 (2021) 106386. <https://doi.org/10.1016/j.cemconres.2021.106386>.
112. J.G. Sanjayan, B. Nematollahi, M. Xia, T. Marchment, Effect of surface moisture on inter-layer strength of 3D printed concrete, *Construction and Building Materials* 172 (2018) 468–475. <https://doi.org/10.1016/j.conbuildmat.2018.03.232>.
113. T. Mader, M. Schreter-Fleischhacker, O. Shkundalova, M. Neuner, G. Hofstetter, Constitutive modeling of orthotropic nonlinear mechanical behavior of hardened 3D printed concrete, *Acta Mech* 234 (2023) 5893–5918. <https://doi.org/10.1007/s00707-023-03706-z>.
114. L. Senff, J.A. Labrincha, V.M. Ferreira, D. Hotza, W.L. Repette, Effect of nano-silica on rheology and fresh properties of cement pastes and mortars, *Construction and Building Materials* 23 (2009) 2487–2491. <https://doi.org/10.1016/j.conbuildmat.2009.02.005>.
115. G. Quercia, G. Hüskén, H.J.H. Brouwers, Water demand of amorphous nano silica and its impact on the workability of cement paste, *Cement and Concrete Research* 42 (2012) 344–357. <https://doi.org/10.1016/j.cemconres.2011.10.008>.
116. Q. Yuan, D. Zhou, B. Li, H. Huang, C. Shi, Effect of mineral admixtures on the structural build-up of cement paste, *Construction and Building Materials* 160 (2018) 117–126. <https://doi.org/10.1016/j.conbuildmat.2017.11.050>.
117. Z. Liu, M. Li, G.S.J. Moo, H. Kobayashi, T.N. Wong, M.J. Tan, Effect of Nanostructured Silica Additives on the Extrusion-Based 3D Concrete Printing Application, *J. Compos. Sci.* 7 (2023) 191. <https://doi.org/10.3390/jcs7050191>.
118. J. Kruger, S. Zeranka, G. Van Zijl, An ab initio approach for thixotropy characterisation of (nanoparticle-infused) 3D printable concrete, *Construction and Building Materials* 224 (2019) 372–386. <https://doi.org/10.1016/j.conbuildmat.2019.07.078>.
119. Nanotechnology for Improved Three-Dimensional Concrete Printing Constructability, *MJ* 118 (2021). <https://doi.org/10.14359/51733101>.

120. M. Van Den Heever, F.A. Bester, P.J. Kruger, G.P.A.G. Van Zijl, Effect of silicon carbide (SiC) nanoparticles on 3D printability of cement-based materials, in: A. Zingoni (Ed.), *Advances in Engineering Materials, Structures and Systems: Innovations, Mechanics and Applications*, 1st ed., CRC Press, 2019: pp. 1616–1621. <https://doi.org/10.1201/9780429426506-279>.
121. Q. Jiang, Q. Liu, S. Wu, H. Zheng, W. Sun, Modification effect of nanosilica and polypropylene fiber for extrusion-based 3D printing concrete: Printability and mechanical anisotropy, *Additive Manufacturing* 56 (2022) 102944. <https://doi.org/10.1016/j.addma.2022.102944>.
122. M.S.M. Norhasri, M.S. Hamidah, A.M. Fadzil, Applications of using nano material in concrete: A review, *Construction and Building Materials* 133 (2017) 91–97. <https://doi.org/10.1016/j.conbuildmat.2016.12.005>.
123. A. Douba, S. Ma, S. Kawashima, Rheology of fresh cement pastes modified with nanoclay-coated cements, *Cement and Concrete Composites* 125 (2022) 104301. <https://doi.org/10.1016/j.cemconcomp.2021.104301>.
124. H. Varela, G. Barluenga, A. Perrot, Extrusion and structural build-up of 3D printing cement pastes with fly ash, nanoclays and VMAs, *Cement and Concrete Composites* 142 (2023) 105217. <https://doi.org/10.1016/j.cemconcomp.2023.105217>.
125. S. Kawashima, J.H. Kim, D.J. Corr, S.P. Shah, Study of the mechanisms underlying the fresh-state response of cementitious materials modified with nanoclays, *Construction and Building Materials* 36 (2012) 749–757. <https://doi.org/10.1016/j.conbuildmat.2012.06.057>.
126. S. Kawashima, M. Chaouche, D.J. Corr, S.P. Shah, Rate of thixotropic rebuilding of cement pastes modified with highly purified attapulgite clays, *Cement and Concrete Research* 53 (2013) 112–118. <https://doi.org/10.1016/j.cemconres.2013.05.019>.
127. Y. Wang, Y. Jiang, T. Pan, K. Yin, The Synergistic Effect of Ester-Ether Copolymerization Thixo-Tropic Superplasticizer and Nano-Clay on the Buildability of 3D Printable Cementitious Materials, *Materials* 14 (2021) 4622. <https://doi.org/10.3390/ma14164622>.
128. A.S. Natanzi, C. McNally, Experimental investigation of low carbon 3D printed concrete, *Transportation Research Procedia* 72 (2023) 3696–3702. <https://doi.org/10.1016/j.trpro.2023.11.550>.
129. B. Panda, N.A. Noor Mohamed, S.C. Paul, G. Bhagath Singh, M.J. Tan, B. Šavija, The Effect of Material Fresh Properties and Process Parameters on Buildability and Interlayer Adhesion of 3D Printed Concrete, *Materials* 12 (2019) 2149. <https://doi.org/10.3390/ma12132149>.
130. Y. Zhang, Y. Zhang, W. She, L. Yang, G. Liu, Y. Yang, Rheological and harden properties of the high-thixotropy 3D printing concrete, *Construction and Building Materials* 201 (2019) 278–285. <https://doi.org/10.1016/j.conbuildmat.2018.12.061>.
131. Q. Liu, Q. Jiang, Z. Zhou, J. Xin, M. Huang, The printable and hardened properties of nano-calcium carbonate with modified polypropylene fibers for cement-based 3D printing, *Construction and Building Materials* 369 (2023) 130594. <https://doi.org/10.1016/j.conbuildmat.2023.130594>.
132. Q. Fu, Z. Zhang, X. Zhao, W. Xu, D. Niu, Effect of nano calcium carbonate on hydration characteristics and microstructure of cement-based materials: A review, *Journal of Building Engineering* 50 (2022) 104220. <https://doi.org/10.1016/j.job.2022.104220>.
133. H. Yang, Y. Che, M. Shi, Influences of calcium carbonate nanoparticles on the workability and strength of 3D printing cementitious materials containing limestone powder, *Journal of Building Engineering* 44 (2021) 102976. <https://doi.org/10.1016/j.job.2021.102976>.
134. H. Yang, W. Li, Y. Che, 3D Printing Cementitious Materials Containing Nano-CaCO₃: Workability, Strength, and Microstructure, *Front. Mater.* 7 (2020) 260. <https://doi.org/10.3389/fmats.2020.00260>.
135. X. Sun, Q. Wang, H. Wang, L. Chen, Influence of multi-walled nanotubes on the fresh and hardened properties of a 3D printing PVA mortar ink, *Construction and Building Materials* 247 (2020) 118590. <https://doi.org/10.1016/j.conbuildmat.2020.118590>.
136. G. Goracci, D. Salgado, J. Gaitero, J. Dolado, Electrical Conductive Properties of 3D-Printed Concrete Composite with Carbon Nanofibers, *Nanomaterials* 12 (2022) 3939. <https://doi.org/10.3390/nano12223939>.
137. M. Kosson, L. Brown, F. Sanchez, Early-Age Performance of 3D Printed Carbon Nanofiber and Carbon Microfiber Cement Composites, *Transportation Research Record* 2674 (2020) 10–20. <https://doi.org/10.1177/0361198120902704>.

138. K. Ahmadi, S.S. Mousavi, M. Dehestani, Influence of nano-coated micro steel fibers on mechanical and self-healing properties of 3D printable concrete using graphene oxide and polyvinyl alcohol, *Journal of Adhesion Science and Technology* 38 (2024) 1312–1333. <https://doi.org/10.1080/01694243.2023.2253623>.
139. A. Dulaj, T.A.M. Salet, S.S. Lucas, Mechanical properties and self-sensing ability of graphene-mortar compositions with different water content for 3D printing applications, *Materials Today: Proceedings* 70 (2022) 412–417. <https://doi.org/10.1016/j.matpr.2022.09.278>.
140. R.H. Rosa, R.S. Silva, L.L. Nascimento, M.H. Okura, A.O.T. Patrocinio, J.A. Rossignolo, Photocatalytic and Antimicrobial Activity of TiO₂ Films Deposited on Fiber-Cement Surfaces, *Catalysts* 13 (2023) 861. <https://doi.org/10.3390/catal13050861>.
141. H. Dikkar, V. Kapre, A. Diwan, S.K. Sekar, Titanium dioxide as a photocatalyst to create self-cleaning concrete, *Materials Today: Proceedings* 45 (2021) 4058–4062. <https://doi.org/10.1016/j.matpr.2020.10.948>.
142. B. Zahabizadeh, I.R. Segundo, J. Pereira, E. Freitas, A. Camões, C.J. Tavares, V. Teixeira, V.M.C.F. Cunha, M.F.M. Costa, J.O. Carneiro, Development of Photocatalytic 3D-Printed Cementitious Mortars: Influence of the Curing, Spraying Time Gaps and TiO₂ Coating Rates, *Buildings* 11 (2021) 381. <https://doi.org/10.3390/buildings11090381>.
143. B. Zahabizadeh, I. Rocha Segundo, J. Pereira, E. Freitas, A. Camões, V. Teixeira, M.F.M. Costa, V.M.C.F. Cunha, J.O. Carneiro, Photocatalysis of functionalised 3D printed cementitious materials, *Journal of Building Engineering* 70 (2023) 106373. <https://doi.org/10.1016/j.jobbe.2023.106373>.
144. Q. Liu, Q. Jiang, M. Huang, J. Xin, P. Chen, The fresh and hardened properties of 3D printing cement-base materials with self-cleaning nano-TiO₂: An exploratory study, *Journal of Cleaner Production* 379 (2022) 134804. <https://doi.org/10.1016/j.jclepro.2022.134804>.
145. H.A. Salah, A.A. Mutalib, A.B.M.A. Kaish, A. Syamsir, H.A. Algaifi, Development of Ultra-High-Performance Silica Fume-Based Mortar Incorporating Graphene Nanoplatelets for 3-Dimensional Concrete Printing Application, *Buildings* 13 (2023) 1949. <https://doi.org/10.3390/buildings13081949>.
146. Y. Che, H. Yang, Hydration products, pore structure, and compressive strength of extrusion-based 3D printed cement pastes containing nano calcium carbonate, *Case Studies in Construction Materials* 17 (2022) e01590. <https://doi.org/10.1016/j.cscm.2022.e01590>.
147. Q. Liu, Q. Jiang, Z. Zhou, J. Xin, M. Huang, The printable and hardened properties of nano-calcium carbonate with modified polypropylene fibers for cement-based 3D printing, *Construction and Building Materials* 369 (2023) 130594. <https://doi.org/10.1016/j.conbuildmat.2023.130594>.
148. P. Xu, T. Chen, K. Fan, M. Zhang, Effect of nano-silica sol dosage on the properties of 3D-printed concrete, *Journal of Building Engineering* 80 (2023) 108090. <https://doi.org/10.1016/j.jobbe.2023.108090>.
149. Q. Jiang, Q. Liu, S. Wu, H. Zheng, W. Sun, Modification effect of nanosilica and polypropylene fiber for extrusion-based 3D printing concrete: Printability and mechanical anisotropy, *Additive Manufacturing* 56 (2022) 102944. <https://doi.org/10.1016/j.addma.2022.102944>.
150. S. Kanagasuntharam, S. Ramakrishnan, J. Sanjayan, Investigating PCM encapsulated NaOH additive for set-on-demand in 3D concrete printing, *Cement and Concrete Composites* 145 (2024) 105313. <https://doi.org/10.1016/j.cemconcomp.2023.105313>.
151. A. Douba, S. Ma, S. Kawashima, Rheology of fresh cement pastes modified with nanoclay-coated cements, *Cement and Concrete Composites* 125 (2022) 104301. <https://doi.org/10.1016/j.cemconcomp.2021.104301>.
152. U. Kilic, J. Ma, E. Baharlou, O.E. Ozbulut, Effects of viscosity modifying admixture and nanoclay on fresh and rheo-viscoelastic properties and printability characteristics of cementitious composites, *Journal of Building Engineering* 70 (2023) 106355. <https://doi.org/10.1016/j.jobbe.2023.106355>.
153. E.M. Aydin, B. Kara, Z.B. Bundur, N. Ozyurt, O. Bebek, M. Ali Gulgun, A comparative evaluation of sepiolite and nano-montmorillonite on the rheology of cementitious materials for 3D printing, *Construction and Building Materials* 350 (2022) 128935. <https://doi.org/10.1016/j.conbuildmat.2022.128935>.
154. G. Sun, Z. Wang, C. Yu, X. Qian, R. Chen, X. Zhou, Y. Weng, Y. Song, S. Ruan, Properties and microstructures of 3D printable sulphaaluminate cement concrete containing industrial by-products and nano clay, *Journal of Building Engineering* 73 (2023) 106839. <https://doi.org/10.1016/j.jobbe.2023.106839>.

155. I. Dejaeghere, M. Sonebi, G. De Schutter, Influence of nano-clay on rheology, fresh properties, heat of hydration and strength of cement-based mortars, *Construction and Building Materials* 222 (2019) 73–85. <https://doi.org/10.1016/j.conbuildmat.2019.06.111>.
156. C. Moro, V. Francioso, M. Velay-Lizancos, Modification of CO₂ capture and pore structure of hardened cement paste made with nano-TiO₂ addition: Influence of water-to-cement ratio and CO₂ exposure age, *Construction and Building Materials* 275 (2021) 122131. <https://doi.org/10.1016/j.conbuildmat.2020.122131>.
157. V. Vishwakarma, S. Uthaman, Environmental impact of sustainable green concrete, in: *Smart Nanoconcretes and Cement-Based Materials*, Elsevier, 2020: pp. 241–255. <https://doi.org/10.1016/B978-0-12-817854-6.00009-X>.
158. H. Monteiro, B. Moura, N. Soares, Advancements in nano-enabled cement and concrete: Innovative properties and environmental implications, *Journal of Building Engineering* 56 (2022) 104736. <https://doi.org/10.1016/j.jobe.2022.104736>.
159. M. Khasreen, P.F. Banfill, G. Menzies, Life-Cycle Assessment and the Environmental Impact of Buildings: A Review, *Sustainability* 1 (2009) 674–701. <https://doi.org/10.3390/su1030674>.
160. L. Rincón, A. Castell, G. Pérez, C. Solé, D. Boer, L.F. Cabeza, Evaluation of the environmental impact of experimental buildings with different constructive systems using Material Flow Analysis and Life Cycle Assessment, *Applied Energy* 109 (2013) 544–552. <https://doi.org/10.1016/j.apenergy.2013.02.038>.
161. D. Kellenberger, H.-J. Althaus, Relevance of simplifications in LCA of building components, *Building and Environment* 44 (2009) 818–825. <https://doi.org/10.1016/j.buildenv.2008.06.002>.
162. S. Bhattacharjee, A.S. Basavaraj, A.V. Rahul, M. Santhanam, R. Gettu, B. Panda, E. Schlangen, Y. Chen, O. Copuroglu, G. Ma, L. Wang, M.A. Basit Beigh, V. Mechtcherine, Sustainable materials for 3D concrete printing, *Cement and Concrete Composites* 122 (2021) 104156. <https://doi.org/10.1016/j.cemconcomp.2021.104156>.
163. A.W. Carpenter, C.-F. De Lannoy, M.R. Wiesner, Cellulose Nanomaterials in Water Treatment Technologies, *Environ. Sci. Technol.* 49 (2015) 5277–5287. <https://doi.org/10.1021/es506351r>.
164. G.K. Dolgun, M. Koşan, M. Kayfeci, A.G. Georgiev, A. Keçebaş, Life Cycle Assessment and Cumulative Energy Demand Analyses of a Photovoltaic/Thermal System with MWCNT/Water and GNP/Water Nanofluids, *Processes* 11 (2023) 832. <https://doi.org/10.3390/pr11030832>.
165. R.S. Dubey, K.V. Krishnamurthy, S. Singh, Experimental studies of TiO₂ nanoparticles synthesized by sol-gel and solvothermal routes for DSSCs application, *Results in Physics* 14 (2019) 102390. <https://doi.org/10.1016/j.rinp.2019.102390>.
166. P. Zhai, J.A. Isaacs, M.J. Eckelman, Net energy benefits of carbon nanotube applications, *Applied Energy* 173 (2016) 624–634. <https://doi.org/10.1016/j.apenergy.2016.04.001>.
167. S.C. Carroccio, P. Scarfato, E. Bruno, P. Aprea, N.T. Dintcheva, G. Filippone, Impact of nanoparticles on the environmental sustainability of polymer nanocomposites based on bioplastics or recycled plastics – A review of life-cycle assessment studies, *Journal of Cleaner Production* 335 (2022) 130322. <https://doi.org/10.1016/j.jclepro.2021.130322>.
168. P. Martens, M. Mathot, F. Bos, J. Coenders, Optimising 3D Printed Concrete Structures Using Topology Optimisation, in: D.A. Hordijk, M. Luković (Eds.), *High Tech Concrete: Where Technology and Engineering Meet*, Springer International Publishing, Cham, 2018: pp. 301–309. https://doi.org/10.1007/978-3-319-59471-2_37.
169. A. Liew, D.L. López, T. Van Mele, P. Block, Design, fabrication and testing of a prototype, thin-vaulted, unreinforced concrete floor, *Engineering Structures* 137 (2017) 323–335. <https://doi.org/10.1016/j.engstruct.2017.01.075>.
170. S.T. Bukhari, S.Q. Bukhari, M. Fahad, Sustainability evaluation of home appliance industry in Pakistan, in: F.M. Da Silva, H. Bártolo, P. Bártolo, R. Almendra, F. Roseta, H.A. Almeida, A.C. Lemos (Eds.), *Challenges for Technology Innovation: An Agenda for the Future*, 1st ed., CRC Press, 2017: pp. 233–235. <https://doi.org/10.1201/9781315198101-41>.
171. K. Heywood, P. Nicholas, Sustainability and 3D concrete printing: identifying a need for a more holistic approach to assessing environmental impacts, *ARIN* 2 (2023) 12. <https://doi.org/10.1007/s44223-023-00030-3>.

172. T. Wangler, E. Lloret, L. Reiter, N. Hack, F. Gramazio, M. Kohler, M. Bernhard, B. Dillenburger, J. Buchli, N. Roussel, R. Flatt, Digital Concrete: Opportunities and Challenges, RILEM Tech Lett 1 (2016) 67–75. <https://doi.org/10.21809/rilemtechlett.2016.16>.
173. N. Labonnote, A. Rønnquist, B. Manum, P. Rüther, Additive construction: State-of-the-art, challenges and opportunities, Automation in Construction 72 (2016) 347–366. <https://doi.org/10.1016/j.autcon.2016.08.026>.
174. N. Hack, T. Wangler, J. Mata-Falcón, K. Dörfler, N. Kumar, A. Walzer, K. Graser, L. Reiter, H. Richner, J. Buchli, W. Kaufmann, R. Flatt, F. Gramazio, M. Kohler, MESH MOULD: AN ON SITE, ROBOTICALLY FABRICATED, FUNCTIONAL FORMWORK, 2017.
175. G. Habert, D. Arribe, T. Dehove, L. Espinasse, R. Le Roy, Reducing environmental impact by increasing the strength of concrete: quantification of the improvement to concrete bridges, Journal of Cleaner Production 35 (2012) 250–262. <https://doi.org/10.1016/j.jclepro.2012.05.028>.
176. I. Agustí-Juan, G. Habert, Environmental design guidelines for digital fabrication, Journal of Cleaner Production 142 (2017) 2780–2791. <https://doi.org/10.1016/j.jclepro.2016.10.190>.

Disclaimer/Publisher's Note: The statements, opinions and data contained in all publications are solely those of the individual author(s) and contributor(s) and not of MDPI and/or the editor(s). MDPI and/or the editor(s) disclaim responsibility for any injury to people or property resulting from any ideas, methods, instructions or products referred to in the content.